The Thesis Committee for Jong Suk Kim

Certifies that this is the approved version of the following thesis:

Development of Linear Capacitance-Resistance Models for Characterizing Waterflooded Reservoirs

APPROVED BY
SUPERVISING COMMITTEE:

Supervisor:

Thomas F. Edgar

Co-Supervisor:

Larry W. Lake

Development of Linear Capacitance-Resistance Models for Characterizing Waterflooded Reservoirs

by

Jong Suk Kim, B.S. Chem. Eng.

Thesis

Presented to the Faculty of the Graduate School of

The University of Texas at Austin

in Partial Fulfillment

of the Requirements

for the Degree of

Master of Science in Engineering

The University of Texas at Austin

December 2011

Dedication

To my parents, sisters, and friends

Acknowledgments

First and foremost, I would like to thank my supervisors Dr. Thomas F. Edgar and Dr. Larry W. Lake for their help in guiding me through this work at the University of Texas at Austin. It was a great opportunity and a pleasure to be able to work with them. Their patient efforts and encouragement on my behalf are sincerely appreciated. I am also thankful to Dr. Leon Lasdon for his suggestions and support on this work.

The faculty and staff of the Chemical Engineering Department and the Petroleum and Geosystems Engineering Department at the University of Texas at Austin were helpful and supportive during my time here. Special thanks to T stockman, Kay Costales-Swift, Sarah D. Berry-Caperton, Allison B. Brooks, Randy Rife, and Patrick Danielewski for their efforts.

I would also like to thank the Computer Modeling Group Ltd. (CMG) for permission to use their reservoir simulation software in this work.

I was supported financially be the members of the Center for Petroleum Asset Risk Management (CPARM) of the University of Texas at Austin. Their support is gratefully acknowledged. Special thanks to Mr. Emilio Nunez for his help and guidance.

I am grateful for the association with the members of Dr. Edgar's research group here at the University of Texas at Austin including: Ninad Patwardhan, Ela Joag, Doug French, Xialjing Jiang, Ramiro Palma, Kriti Kapoor, Kody Powell, Vinay Kumar, Wesley Cole, Akshay Sriprasad, Dr. Ricardo Dunia, Dr. Ben Spivey, Dr. Bhalinder S.

Gill, and Dr. Ivan Castillo. Their help and support is appreciated. I would also like to recognize the contribution of Anh Nguyen who also worked on this project.

Finally, I am most grateful for the love, encouragement, understanding and support of my parents and sisters. This work is a tribute to their sacrifice.

Jong Suk Kim

December 2011

Abstract

Development of Linear Capacitance-Resistance Models for Characterizing Waterflooded Reservoirs

by

Jong Suk Kim, M.S.E.

The University of Texas at Austin, 2011

Supervisor: Thomas F. Edgar

Co-Supervisor: Larry W. Lake

The capacitance-resistance model (CRM) has been continuously improved and tested on both synthetic and real fields. For a large waterflood, with hundreds of injectors and producers present in a reservoir, tens of thousands of model parameters (gains, time constants, and productivity indices) in a field must be determined to completely define the CRM. In this case obtaining a unique solution in history-matching large reservoirs by nonlinear regression is difficult. Moreover, this approach is more likely to produce parameters that are statistically insignificant. The nonlinear nature of the CRM also makes it difficult to quantify the uncertainty in model parameters.

The analytical solutions of the two linear reservoir models, the linearly transformed CRM whose control volume is the drainage volume around each producer

(*lt*CRMP) and integrated capacitance-resistance model (ICRM), are developed in this work. Both models are derived from the governing differential equation of the producer-based representation of CRM (CRMP) that represents an in-situ material balance over the effective pore volume of a producer. The proposed methods use a constrained linear multivariate regression (LMR) to provide information about preferential permeability trends and fractures in a reservoir. The two models' capabilities are validated with simulated data in several synthetic case studies.

The *lt*CRMP and ICRM have the following advantages over the nonlinear waterflood model (CRMP): (1) convex objective functions, (2) elimination of the use of solver when constraints are ignored, and (3) faster computation time in optimization. In both methods, a unique solution can always be obtained regardless of the number of parameters as long as the number of data points is greater than the number of unknowns (parameters). The methods of establishing the confidence limits on CRMP gains and ICRM parameters are demonstrated in this work.

This research also presents a method that uses the ICRM to estimate the gains between newly introduced injectors and existing producers for a homogeneous reservoir without having to do additional simulations or regression on newly simulated data. This procedure can guide geoscientists to decide where to drill new injectors to increase future oil recovery and provide rapid solutions without having to run reservoir simulations for each scenario.

Table of Contents

List of Tables

List of Figures

Chapter 1: Introduction

As conventional oil supplies are becoming more limited, evaluating a reservoir characteristics and predicting future production performance have become very important tasks. To achieve these tasks, reservoir engineers must choose an adequate method, which could be empirical, analytical, or numerical, to model past reservoir behavior and use this model to forecast future reservoir production. After choosing the right model for a particular application, one can determine the optimal oil production strategy, e.g., optimal water injection scheme for a secondary recovery, which would maximize the net present value (NPV) of the reservoir asset.

Traditional reservoir simulators can provide reasonable solutions if accurate input data on reservoir properties are used for simulation runs; however, collecting the required reservoir input data is time-consuming and costly. Moreover, complex numerical simulations are computationally prohibitive to use when simulations involve millions of grid blocks and hundreds of wells for a very large reservoir. Therefore, the need for simplified reservoir models that can provide rapid prediction of future recovery and reservoir performance has been growing.

1.1 Waterflooding Predictive Models

Secondary-recovery operations are those of injection of fluids (gas, air, or water) after the reservoir has reached a state of substantially complete depletion of its initial content of energy available for oil expulsion or where the production rates have

approached the limits of profitable operation (Walsh and Lake, 2003). In secondary recovery, the most common injectant is water. Buckley and Leverett (1942) proposed a simple simulation method that calculates fractional flow and recovery performance after water breakthrough for a linear reservoir with homogeneous properties. Welge (1952) extended the frontal advance theory proposed by Buckley and Leverett. Stiles (1949) and Dykstra-Parsons (1950) developed simple methods for calculating recovery in stratified homogeneous reservoirs. These methods are based on the assumption of a piston-like displacement of oil in a linear bed, and Stiles showed that the rate of advance of flood front is proportional to the permeability of the bed. However, the assumptions made on these models are too simple to be used in field cases where the heterogeneity of the reservoir has a great effect on reservoir production.

Heffer et al. (1995) used the Spearman rank coefficient to estimate injector-producer relationships based on autocorrelation between injection and production rates. Refunjol (1996) introduced time delays in the correlation analysis, and De Sant' Anna Pizarro (1998) validated this technique with numerical simulations. Soeriawinata and Kelkar (1999) extended the Spearman rank correlation method by incorporating the superposition effect in the reservoir caused by the influence of multiple injection wells on a producing well, and Barros-Griffiths (1998) validated this technique using tracer tests in an actual field. Panda and Chopra (1998) used artificial neural networks to determine the interaction between injector/producer pairs. In this approach, wells (equivalent to nodes in a neural network) are related by mathematical weights. The network should be trained using historic data such as water injection rates and oil and water production rates.

Because of the rapid advances made in computer hardware and software technology, numerical simulation has become the dominant method to model past reservoir behavior and to forecast future reservoir production. Reservoir simulation allows a more detailed study of the reservoir by dividing the reservoir into a number of blocks and applying fundamental equations for flow in porous media to each block (Aziz and Settari, 1979). However, the differential equations governing the physical flow into and out of each grid block must be solved by using the finite difference method. This could become computationally expensive when a reservoir is so large that it involves millions of grid blocks in simulations. Furthermore, conventional reservoir simulators require a priori data to be specified before running simulations such as geologic and fluid properties.

Albertoni and Lake (2003) estimated the connectivity between injector/producer well pairs on the basis of a linear model with coefficients calculated by multiple linear regression (MLR). Estimated regression coefficients quantitatively indicate the communication between injector/producer well pairs in a waterflooded reservoir. The time lag between a producer and an injector was accounted for by filters.

Yousef et al. (2006) introduced the capacitance model (CM) that can quantify interwell connectivity and the degree of fluid storage (compressibility) between well pairs. The CM provides the same information as the Spearman rank correlation models but is derived from a physical model of the reservoir fluids. Sayarpour et al. (2007) introduced analytical solutions of the fundamental differential equation of the CM based on superposition in time and developed model structures for different reservoir control

volumes. Weber et al. (2009) used the capacitance-resistance model (CRM) to optimize injection allocation and well location in waterfloods with many variables and constraints.

1.2 Research Objective and Overview of Thesis

The objectives of this research are to develop and apply linearized capacitance-resistance models to waterfloods and to evaluate the uncertainty of estimated model parameters. Also, the relationship between interwell-connectivities and interwell-distance between injector-producer well-pairs is investigated.

Section 1.1 gave a literature review surveying waterflooding predictive models. Chapter 2 reviews the theory and derivation of producer-based representation of capacitance-resistance model (CRM). This chapter also contains the derivations of two linear capacitance-resistance models, the linearly transformed CRMP (*lt*CRMP) and integrated capacitance-resistance model (ICRM), and they are compared to the CRMP.

Chapter 3 presents the validation and application of the three simple reservoir models discussed in Chapter 2 on several synthetic oil fields in which there are five injectors and four producers. Conventional reservoir simulators, such as Eclipse and the Implicit-Explicit black oil simulator (IMEX) developed by Computer Model Group Ltd. (CMG), were used to generate synthetic field data. The relationship between interwell-connectivities and interwell-distance between well-pairs was also investigated in Chapter 3.

Chapter 4 discusses uncertainty quantification of the model parameters. Statistical techniques that determine confidence limits on the model estimates were presented.

Finally, Chapter 5 summarizes the key contributions of this research and presents recommendations for future work.

Chapter 2: Simple Reservoir Models for Secondary Recovery

Conventional reservoir simulators such as Eclipse and the IMEX solve the differential material balance equations numerically to calculate the pressure and oil saturation of each grid block in the reservoir. However, these values (pressure and oil saturation) not only vary spatially from one grid block to another but also vary over time requiring them to be updated as simulation progresses. This could be very cumbersome process when a large reservoir needs to be modeled because large simulations involve a millions of grid blocks. Collecting core samples to estimate rock and fluid properties, which are the necessary input data to run reservoir simulators, is also time-consuming and costly job. As a result of these issues encountered in traditional reservoir simulations, simple reservoir models have become more attractive to reservoir engineers.

In this chapter, the background and development of the capacitance-resistance model (CRM) is demonstrated. The linearly transformed CRMP (*lt*CRMP) and integrated capacitance-resistance model (ICRM) that are alternative models to CRMP applicable for secondary recovery were developed in this research. Three simple reservoir models were compared to each other in the following sections.

2.1 Capacitance-Resistance Model (CRM)

The capacitance-resistance model (CRM) is an input-output model that characterizes the properties of an oil reservoir using only data available at the wells (Weber, 2009). The name CRM is selected for this model because of its analogy to a

resistance-capacitor (RC) circuit (Thompson, 2006). A production rate response to a step-change in injection rate is analogous to voltage measurement of a capacitor in a parallel RC circuit where the battery potential is equivalent to the injection signal (Sayarpour, 2008).

The CRM estimates two types of model parameters via multivariate nonlinear regression: connectivities (or gains) that represent the degree of communication between injector-producer well pairs and time constants that represent the degree of fluid storage (compressibility) or pressure dissipation between well pairs.

2.1.1 CRM Background and History

In secondary recovery, CRM has been continuously improved and tested on both synthetic and real oil fields, and the validity and capability of the modeling approach have been verified previously by researchers at the University of Texas at Austin. Albertoni and Lake (2003) quantitatively calculated the interwell connectivity between injector-producer well pairs in a waterflooded reservoir by multivariate linear regression with diffusivity filters. Yousef et al. (2006) proposed the capacitance model (CM) and replaced the diffusivity filter that accounts for the time lag between a producer and an injector with a time constant. Two different approaches, the balanced capacitance model (BCM) and the unbalanced capacitance model (UCM), were proposed to study interwell connectivities depending on whether the waterflood is balanced or not. Sayarpour et al. (2007) solved fundamental differential equation of the CM analytically based on superposition in time and developed model structures for three different reservoir control

volumes: 1) volume of the entire field or tank model (CRMT), 2) drainage volume of each producer (CRMP), and 3) drainage volume between each injector-producer pair (CRMIP). Weber (2009) discretized the CRM and used the CRM to optimize injection allocation and well location in waterfloods with many variables and constraints. Nguyen et al. (2011) developed an integrated capacitance-resistance model (ICRM) that uses cumulative water injection and cumulative total production instead of water injection rate and total production rate. The ICRM performs linear multivariate regression (LMR) to obtain the model estimates. Compared to traditional reservoir simulators, the CM, CRM, and ICRM provide a rapid evaluation of reservoir behavior between injectors and producers because three models only require water injection rates (or cumulative water injection) and total liquid production rates (or cumulative total liquid production), which are typically already measured and collected, and producer bottom hole pressure (BHPs) to solve for model parameters. None of the three models require extensive geologic models.

In chemical engineering, the CRM is analogous to a single (or a series of) first-order tank storage model(s), where the flow rate into the tank is used to predict the level of the incompressible fluid inside and the outflow rate (Seborg et al., 2010). Figure 2.1 shows a schematic of how the total production of a slightly compressible fluid (oil and water production) responds to a step-change made on an injection rate in the CRM. The shape of the output response caused by a step-change in injection rate depends on the time lag and attenuation between a producer and an injector.

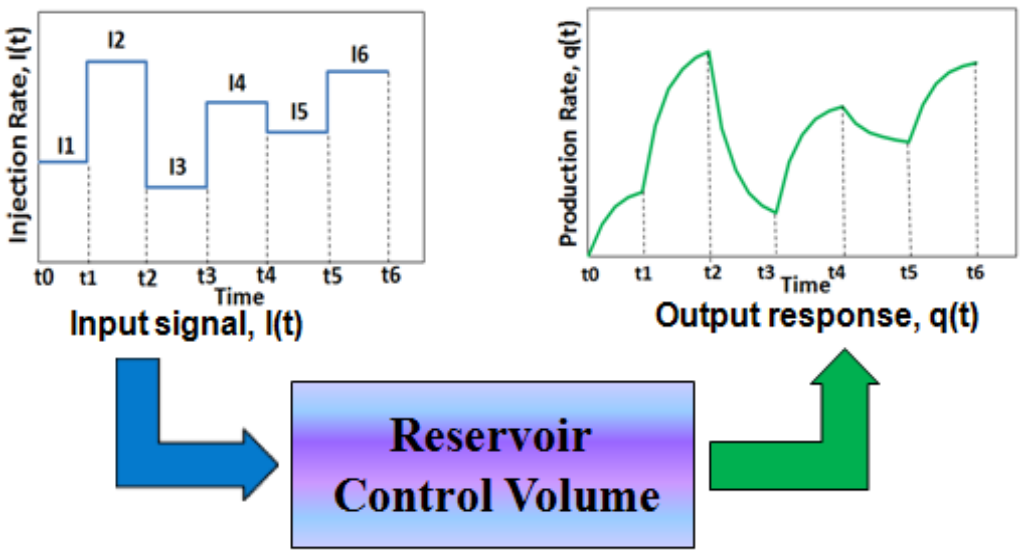

Figure 2.1: Schematic representation of the impact of an injection rate signal on total production response for an arbitrary reservoir control volume in the CRM (Sayarpour, 2008).

2.1.2 Mathematical Derivation of the CRMP

The CRM gives different solutions for different reservoir control volumes. The schematic representation of the CRMP, whose control volume is the drainage volume around each producer, is shown in Figure 2.2.

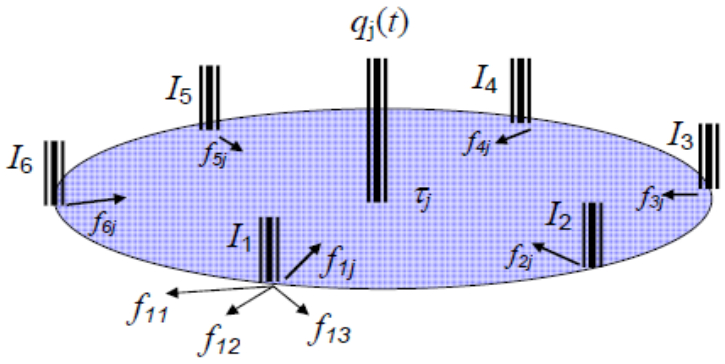

Figure 2.2: Schematic representation of a drainage volume around a single producer used in CRMP (Weber, 2009).

A governing material balance differential equation at reservoir conditions with multiple injectors and one producer j is given as the following:

$$\left(c_t V_P\right)_j \frac{d\bar{p}_j(t)}{dt} = \sum_{i=1}^{N_i} f_{ij} i_i(t) - q_j(t) \tag{2.1}$$

where

N_i is the total number of injectors

c_t is the total compressibility of the reservoir

V_p is the reservoir pore volume

$\bar{p}(t)$ is the average pressure in the reservoir at time t

$i_i(t)$ is the water injection rate of an injector i at time t, and

$q_j(t)$ is the total production (both oil and water) rate from a producer j at time t.

In Equation 2.1, f_{ij} is a well connectivity between a injector i and a producer j. f_{ij} is also called a *gain*. Physically, f_{ij} represents the fraction of water rate from injector i flowing towards producer j at steady state. With the productivity index J defined by Walsh and Lake (2003), a linear productivity model for a producer j is defined as

$$q_j(t) = J_j\left(\bar{p}_j(t) - p_{wf,j}(t)\right) \tag{2.2}$$

where J is the productivity index and $p_{wf}(t)$ is the bottom hole pressure at time t. Substituting Equation 2.2 into Equation 2.1 eliminate the average reservoir pressure, $\bar{p}$, yields the following:

$$q_j(t) = \sum_{i=1}^{N_i} f_{ij} i_i(t) - \left(\frac{c_t V_P}{J}\right)_j \frac{dq_j(t)}{dt} - \left(c_t V_P\right)_j \frac{dp_{wf,j}(t)}{dt} \tag{2.3}$$

Equation 2.3 is the governing differential equation for the CRMP (Liang et al., 2007). The time constant, τ, is defined as

$$\tau = \frac{c_t V_P}{J} \tag{2.4}$$

and Equation 2.3 can be expressed as

$$q_j(t) = \sum_{i=1}^{N_i} f_{ij} i_i(t) - \tau_j \frac{dq_j(t)}{dt} - J_j \tau_j \frac{dp_{wf,j}(t)}{dt} \tag{2.5}$$

Physically, the time constant represents the pressure dissipation or degree of fluid storage (compressibility) between injector/producer well pairs. Equation 2.5 is developed for a system based on the following assumptions (Sayarpour, 2008):

- No new wells are drilled in the field over the analyzed period
- Constant fluid (compressibility, viscosity, density, and etc.) and rock (permeability, porosity, and etc.) properties
- Reservoir temperature is constant or does not vary significantly
- Two immiscible phases coexist
- Capillary pressure and gravity effects are neglected
- Darcy's law applies, and
- Productivity index is constant.

If we assume the injection rates of all injectors are constant and the producer bottom hole pressure varies linearly over a discrete time period, Δt, then Equation 2.5 can be integrated analytically and gives the following solution (the CRMP) for the total production rate of producer *j* in time period k:

$$q_{jk} = q_{j(k-1)} e^{-\Delta t/\tau_j} + \left(1 - e^{-\Delta t/\tau_j}\right)\left(\sum_{i=1}^{N_i} f_{ij} i_{ik} - J_j \tau_j \frac{p_{wf,j}^{k} - p_{wf,j}^{k-1}}{\Delta t}\right) \tag{2.6}$$

In Equation 2.6, q_{jk} is a weighted sum of the previous total production rate in time period k-1, $q_{j(k-1)}$, and the combined effect of the current rate of arrival of water at the producer j from all injectors and producer BHP change at the well.

The CRMP only requires field production data to infer the interwell connectivity between well pairs. Also, the CRMP allows the rapid estimation of future production rates of the producer j at any injection rates and producer BHPs if model parameters are specified. If producer BHPs are constant, Equation 2.6 can be simplified (Equation 2.7):

$$q_{jk} = q_{j(k-1)} e^{-\Delta t/\tau_j} + \left(1 - e^{-\Delta t/\tau_j}\right)\sum_{i=1}^{N_i} f_{ij} i_{ik} \tag{2.7}$$

In Equation 2.7, model parameters such as the gains, time constants, and the productivity indices are estimated by nonlinear multivariate regression that minimizes the following objective function:

$$\min z = \sum_{k=1}^{n_t}\sum_{j=1}^{n_p}\left(\left(q_{jk}\right)_{obs} - \left(q_{jk}\right)_{cal}\right)^2 \tag{2.8}$$

where $(q_{jk})_{obs}$ is the observed total production rate, $(q_{jk})_{cal}$ is the calculated total production rate by the model, n_p is the total number of producers, and n_t is the total number of historic time periods selected in a fitting window. This objective function is solved with Equation 2.7 (if producer BHPs are constant) as well as additional constraints:

$$\sum_{j=1}^{n_p} f_{ij} \le 1 \text{ for all } i \tag{2.9}$$

$$f_{ij}, \tau_j \geq 0 \text{ for all } i \text{ and } j \tag{2.10}$$

Equation 2.9 is a total material balance (continuity) allowing for a loss of water injected within the control volume when the sum of *gains* is less than one (Weber et al., 2009). Equation 2.10 ensures that injected water does not adversely affect the reservoir production.

Note that both Equations 2.6 and 2.7 are defined for each producer *j*, but the gains in Equation 2.9 are summed over the injector index *i*. Due to the presence of the constraint (Equation 2.9), it is not possible to minimize the terms in Equations 2.6 and 2.7 corresponding to each producer *j* separately when solving the objective function (Equation 2.8).

2.1.3 Linearly Transformed CRMP (*lt*CRMP)

The CRM is highly nonlinear in the parameters such that it not only has the exponential terms but also is written in a recursive form. What the CRM is expressed in a recursive form means that in order to calculate the production rate at time step k (q_k) by the model, the production rate at time step k-1 (q_{k-1}) needs to be known ahead of time. However, q_{k-1} also depends on the rate at time step k-2 (q_{k-2}). Due to the nonlinear nature of the CRM, it would be difficult to obtain a unique solution in history-matching large reservoirs by nonlinear multivariate regression.

A producer-based representation of CRM (CRMP) can be linearized if the predicted total production rate term on the right-hand side of Equation 2.6 is replaced by

the observed (or measured) total production rate. After lumping and redefining the parameters in Equation 2.6, a linearly transformed CRMP (*lt*CRMP) is obtained:

$$\left(q_{jk}\right)_{cal} = q_{j(k-1)obs}e_j + \sum_{i=1}^{N_i} f_{ij}^{'} i_{ik} - J_j^{'}\left(p_{wf,j}^{k} - p_{wf,j}^{k-1}\right) \tag{2.11}$$

The transformed *gain*, f'_{ij}, is called *effective gain* that accounts for the time-dependent effect of *gain* for each well-pair. From the transformed parameters, the original parameters (f_{ij}, τ_j, and J_j) can be calculated by the relationships shown in Table 2.1.

Table 2.1: Relationships between the original and transformed parameters

Transformed parameter	e_j	f'_{ij}	J'_j
Relationship with the original parameter	$e^{-\Delta t/\tau_j}$	$\left(1-e^{-\Delta t/\tau_j}\right) f_{ij}$	$\dfrac{\left(1-e^{-\Delta t/\tau_j}\right) J_j \tau_j}{\Delta t}$

Equation 2.11 further reduces to Equation 2.12 if producer BHPs are constant.

$$\left(q_{jk}\right)_{cal} = q_{j(k-1)obs}e_j + \sum_{i=1}^{N_i} f_{ij}^{'} i_{ik} \tag{2.12}$$

The constraints associated with the *lt*CRMP are the following:

$$\sum_{j=1}^{n_p} \frac{f_{ij}^{'}}{1-e_j} \le 1 \text{ for all } i \tag{2.13}$$

$$f_{ij}^{'} \ge 0 \text{ for all } i \text{ and } j \tag{2.14}$$

$$0 \le e_j \le 1 \text{ for all } j \tag{2.15}$$

*lt*CRMP's transformed model parameters can be estimated by linear multivariate regression that minimizes the same objective function (Equation 2.8). With a linear model, the objective function becomes a convex function.

An attempt to linearize a nonlinear CRMP results in nonlinear constraints (2.13). However, these constraints form a convex set, so any local minimum found in Equation 2.8 is a global minimum. The convexity of the constraints associated with the *lt*CRMP is shown in Appendix A.

2.2 Integrated Capacitance-Resistance Model (ICRM)

The integrated capacitance-resistance model (ICRM) for secondary recovery is developed from the CRMP governing differential equation (Equation 2.3) that represents the in-situ material balance over the effective pore volume of a producer (Sayarpour et al., 2007). After multiplying both sides of Equation 2.3 by dt, Equation 2.3 can be integrated over the time interval from t_0 to t_k:

$$\int_{q_{j0}}^{q_{jk}} dq_{jk} + \frac{1}{\tau_j}\left(\int_{t_0}^{t_k} q_{jk}\,dt\right) = \frac{1}{\tau_j}\left[\sum_{i=1}^{N_i}\left\{ f_{ij}\left(\int_{t_0}^{t_k} i_{ik}\,dt\right)\right\}\right] - J_j\left(\int_{p^0_{wf,j}}^{p^k_{wf,j}} dp^k_{wf,j}\right) \qquad (2.16)$$

After rearranging terms and integrating Equation 2.16, ICRM for a secondary recovery scheme is obtained:

$$N^k_{p,j} = \left(q_{j0} - q_{jk}\right)\tau_j + \sum_{i=1}^{n_i}\left(f_{ij} CWI^k_i\right) + J_j\tau_j\left(p^0_{wf,j} - p^k_{wf,j}\right) \qquad (2.17)$$

Here, $N^k_{p,j}$ represents the cumulative amount of total liquid, oil and water, produced from a producer j at time step k. The parameter CWI^k_i represents the cumulative volume of

water injected into an injector *i* at time step k. If producer BHPs are constant, Equation 2.17 can be simplified (Equation 2.18):

$$N_{p,j}^{k} = \left(q_{j0} - q_{jk}\right)\tau_j + \sum_{i=1}^{n_i}\left(f_{ij} CWI_i^k\right) \tag{2.18}$$

Model parameters (gains, time constants, and productivity indices) are estimated by linear multivariate regression that minimizes the following objective function:

$$\min z = \sum_{k=1}^{n_t}\sum_{j=1}^{n_p}\left(\left(N_{p,j}^{k}\right)_{obs} - \left(N_{p,j}^{k}\right)_{cal}\right)^2 \tag{2.19}$$

This objective function is solved with Equation 2.17 or Equation 2.18 (with constant producer BHPs) as well as additional constraints (Equations 2.9 and 2.10).

As seen in Equations 2.9, 2.10, and 2.18, the ICRM for secondary recovery and the constraints associated with it are all linear, indicating that any local minimum found in Equation 2.19 is a global minimum. Therefore, a unique set of parameters that give a global minimum is obtained when Equation 2.19 is minimized. When the total water injection is approximately equal to the total liquid production, the waterflood is balanced (Sayarpour et al., 2007). In this case, the constraints (Equation 2.9) can be relaxed (ignored), and Equation 2.20 can be solved for each producer j separately:

$$\min z = \sum_{k=1}^{n_t}\left(\left(N_{p,j}^{k}\right)_{obs} - \hat{N}_{p,j}^{k}\right)^2 \tag{2.20}$$

Furthermore, if all the constraints are ignored, then Equation 2.20 can be solved analytically by matrix inversion.

2.3 Comparison between the CRMP and the ICRM

Although both CRMP and ICRM are developed from the same governing differential equation, their formulations and regression methods are different from one model to another. In this section, the two models are compared and the advantages and disadvantages of each model are discussed.

Both models (CRMP and ICRM) are derived from the first-order ordinary differential equation (Equation 2.3) that describes the flow of the total fluid in oil reservoir. They simplify the reservoir to a system of inputs and outputs. Both models characterize the time-dependent effects of injectors on producers using interwell connetivities and time constants for each input-output pair, similar to linear dynamic models used in chemical process control (Weber et al., 2009). These two models share the following similarities:

- Both models do not require a priori estimation of physical reservoir and fluid properties but only available field data
- They can be used to compute the future water injection rates that maximize the net present value (NPV) of reservoir asset, and
- A regression analysis is performed to estimate the same kinds of model parameters (gains, time constants, and productivity indices) with the same imposing constraints on parameters.

The CRM is used to match total production rates based on changing water injection rates (independent variables). Because the CRM is nonlinear, nonlinear regression is carried out to minimize the objective function.

For a typical large waterflood, hundreds of producers and injectors may be present in a reservoir, resulting in tens of thousands of model parameters in a field to be determined to completely define the CRM. In this case, obtaining a unique solution in history-matching large reservoirs by nonlinear multivariate regression can be difficult, and this approach can produce parameters that are statistically insignificant (Weber et al., 2009). Furthermore, establishing confidence intervals of the model parameters is also difficult because of the nonlinear nature of both models.

The ICRM is purely linear (both the model and constraints) and fits cumulative total productions with cumulative water injections. This model performs linear regression to obtain the model estimates. Therefore with ICRM confidence intervals of model parameters can easily be established (Montgomery and Peck, 1982). Uncertainty quantification of the ICRM's parameters is studied in Chapter 4. The objective function minimized with the ICRM is a convex function. Because the constraints associated with the ICRM are linear as well, any local minimum found by its objective function is a global minimum. As a result of convex optimization, the ICRM guarantees a unique solution regardless of the number of parameters as long as the number of data points is greater than the number of unknowns (parameters). Another advantage of using the ICRM over the CRMP is that the ICRM can be solved analytically by matrix inversion if constraints are relaxed (ignored). Finally, the simpler formulation of the ICRM would reduce computation time. Table 2.2 shows the comparison between the CRMP and the ICR model.

Table 2.2: Comparison between CRM and ICRM

Features \ Models	**CRMP**	**ICRM**
Regression method	Nonlinear multivariate	Linear multivariate
Linearity of the model	Nonlinear	Linear
Linearity of the constraints	Linear	Linear
Dependent variable	Total production rate, q_{jk}	Cumulative total production, N_{pk}
Independent variables	Water injection rate, i_k Producer BHP, $p_{wf,j}^{\ k}$	Cumulative water injection, CWI_{ik} Producer BHP, $p_{wf,j}^{\ k}$
Estimated parameters	Gains, time constants, productivity indices	Gains and time constants, productivity indices
Convex optimization	Yes	No
Analytical solution	Not possible	Possible if constraints are relaxed
Uniqueness of solution	Possibly local minimum	Global minimum
Direct Estimation of confidence intervals on model parameters	Difficult	Easy
Relative computation time	Slow	Fast

2.4 Summary

In this chapter, the mathematical development of the CRMP was reviewed. The *lt*CRMP was derived, whose constraints are nonlinear but form a convex set. The ICRM that is purely linear for secondary recovery was also derived. The ICRM trains cumulative production data based on changing cumulative water injection data.

The CRM and the ICRM share the similarities: the governing differential equation that describes the flow of the total fluid in oil reservoir, no estimation of reservoir and fluid properties required before simulations, and same types and number of model

parameters. Although the two models share a few similarities, the ICRM has many advantages over the CRMP:

- Linear regression analysis can be performed
- Uniqueness of a solution (global minimum) is guaranteed
- Objective function can be solved analytically if constraints are relaxed
- Confidence intervals on model parameters can easily be established, and
- Computation time in optimization is relatively faster.

Chapter 3: Synthetic Case Studies

In this chapter, the ICRM is applied to five synthetic oil fields under waterflooding. The CRMP and *lt*CRMP are also applied to synthetic fields, and the results obtained by applying three models are compared to each other. The numerical simulators (Eclipse and the IMEX) are used to generate synthetic field data on which all three models are fitted. Simulated data are free of noise. The five synthetic oil fields used to validate the models are all undersaturated black-oil reservoirs under waterflooding. The Microsoft Excel Solver is used to solve the objective functions (sum of squared errors between simulated data and calculated values by the models).

3.1 Synfield-1: Streak Case

Synfield-1 is a synthetic oil field (streak case studied by Sayarpour et al., 2007) that consists of five vertical injectors and four vertical producers. Figure 3.1 shows the well locations and permeability distributions of the synthetic field. This streak case is a homogeneous reservoir with porosity of 18% and permeability of 5 md except where the two high-permeability streaks exist. The simulation ran for 100 months of simulated time, and both injectors and producers started operating at the same time (in the first month). The producer BHPs were kept constant at 250 psi for all producers. Figure 3.2 shows the injection history for each injector with water injected for 100 months. Total production rates for each well vs. time are shown in Figure 3.3. In this example, the total water injection was approximately equal to the total liquid production, so the waterflood was

balanced. The numerical simulator Eclipse was used to generate synthetic field data in Synfield-1.

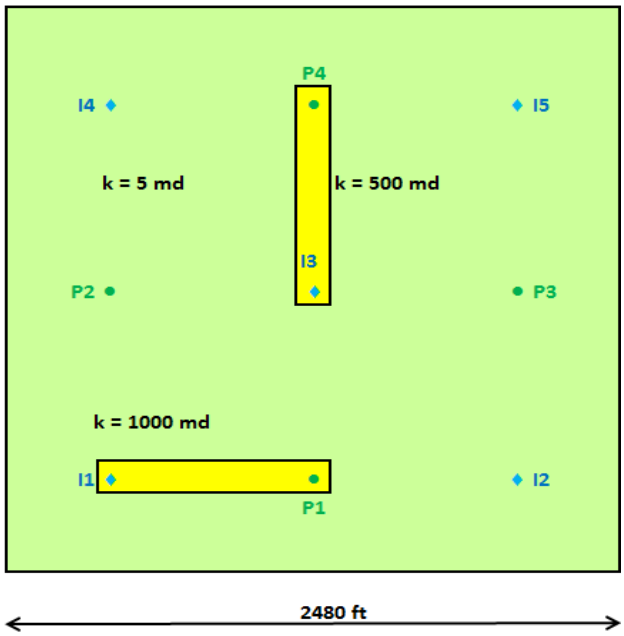

Figure 3.1: Streak case permeability field consists of two high-permeability streaks of 500 and 1,000 md in a field of 5 md (same example as in Liang et al., 2007 and Sayarpour et al., 2007).

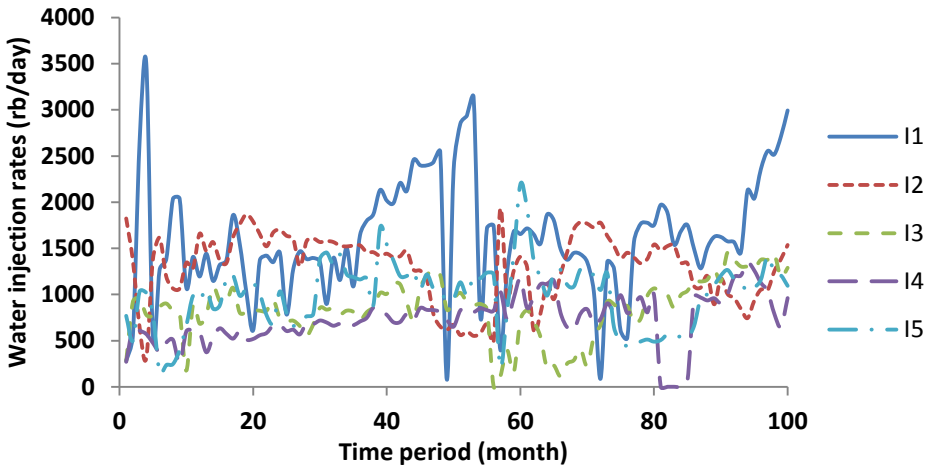

Figure 3.2: Monthly water injection rates of five injectors for the streak case (Albertoni and Lake, 2003).

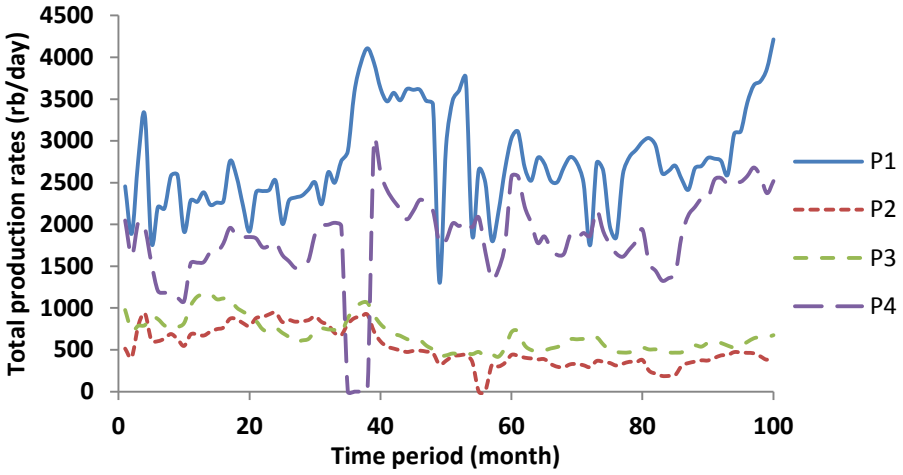

Figure 3.3: Monthly total liquid production rates of four producers in the streak case (Albertoni and Lake, 2003).

3.1.1 CRMP vs. *lt*CRMP

Prior to comparing the two models (CRMP and *lt*CRMP), the sensitivity of the CRMP parameters to relaxing the constraints was examined for the balanced waterflood. The CRMP was applied to match simulated data starting from month 58 to month 100, and the model parameters were estimated by both the unconstrained NMR and the constrained NMR. The results show (see Table 3.1) that the model parameters estimated by the both regression methods are essentially the same, confirming the CRMP parameters are insensitive to relaxing the constraints for the balanced waterflood (Synfield-1). When the constraint (Equations 2.9) was ignored in CRMP optimization, the sum of the gains over all producer indices for I1, I3, and I4 was slightly greater than one, violating the material-balance requirements. However, these values are sufficiently

close to ones to effectively satisfy the material-balance requirements in a waterflooded reservoir.

Table 3.1: Inferred CRMP parameters for the streak case

Unconstrained NMR / Constrained NMR		I1	I2	I3	I4	I5	τ_j (day)
P1	Unconstrained f_{i1}	0.8957	0.5804	0.2241	0.2173	0.1840	15.99
	Constrained f_{i1}	0.8923	0.5822	0.2215	0.2147	0.1891	15.81
P2	Unconstrained f_{i2}	0.0294	0.0328	0.0508	0.2012	0.0394	28.21
	Constrained f_{i2}	0.0265	0.0345	0.0478	0.1985	0.0448	28.13
P3	Unconstrained f_{i3}	0.0198	0.1807	0.0866	0.0348	0.1700	24.16
	Constrained f_{i3}	0.0170	0.1822	0.0835	0.0322	0.1755	24.42
P4	Unconstrained f_{i4}	0.0668	0.1996	0.6504	0.5568	0.5857	21.58
	Constrained f_{i4}	0.0641	0.2011	0.6472	0.5546	0.5907	21.58
$\sum_{j=1}^{n_p} f_{ij}$	Unconstrained	1.012	0.994	1.012	1.010	0.979	
	Constrained	1.000	1.000	1.000	1.000	1.000	

After validating that the CRMP parameters in Synfield-1 were insensitive to relaxing the constraints, both the CRMP and *lt*CRMP methods were applied to match simulated data starting from month 58 to month 100. Equations 2.9 and 2.13 were not used because the waterflood was balanced in streak case.

Table 3.2 shows the transformed model parameters from the *lt*CRMP. Original *lt*CRMP parameters refer CRMP parameters calculated from the resulting *lt*CRMP parameters (or transformed model parameters) by the relationships shown in Table 2.1.

The original *lt*CRMP parameters for the streak case are shown in Table 3.3. Figure 3.4 shows the comparison between the estimated gains from the CRMP and original gains from the *lt*CRMP presented in histograms. The results show the gains estimated from the both models are comparable to each other.

Table 3.2: Inferred *lt*CRMP parameters for the streak case

f'_{ij}	I1	I2	I3	I4	I5	e_j
P1	0.7634	0.4914	0.1917	0.1784	0.1578	0.1504
P2	0.0201	0.0208	0.0337	0.1315	0.0263	0.3415
P3	0.0136	0.1283	0.0619	0.0239	0.1214	0.2906
P4	0.0501	0.1486	0.4885	0.4172	0.4391	0.2507

Table 3.3: Inferred original *lt*CRMP parameters for the streak case

f_{ij}	I1	I2	I3	I4	I5	τ_j (day)
P1	0.8985	0.5784	0.2257	0.2100	0.1857	15.84
P2	0.0306	0.0316	0.0512	0.1996	0.0400	27.92
P3	0.0192	0.1809	0.0873	0.0337	0.1711	24.28
P4	0.0668	0.1984	0.6519	0.5568	0.5860	21.68

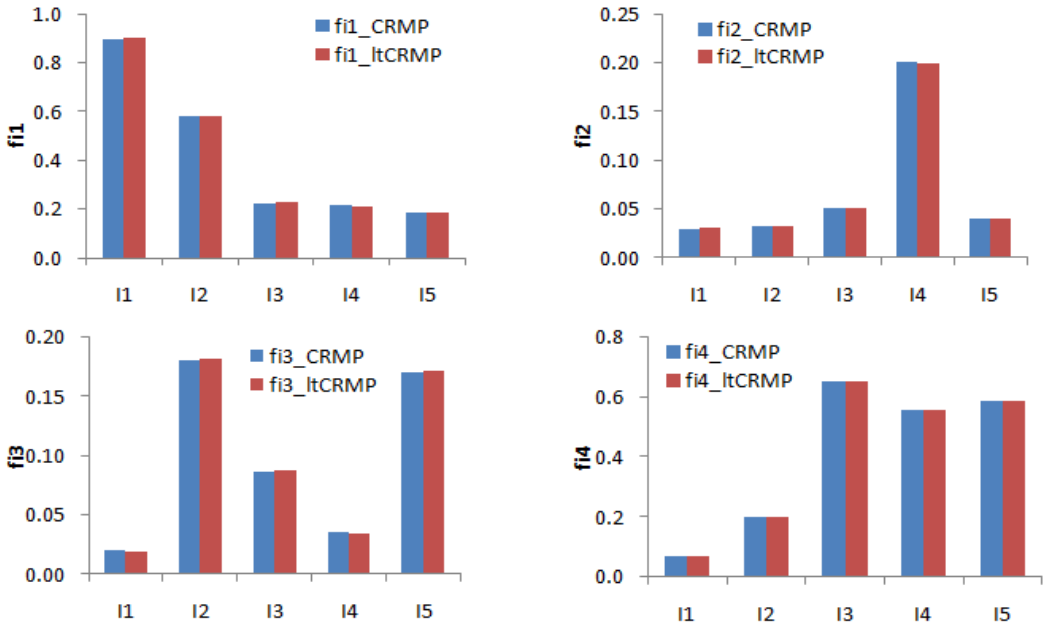

Figure 3.4: Comparison between CRMP gains and original *lt*CRMP gains for P1, P2, P3, and P4 in streak case. Subscript i is an injector index in the range 1 to 5.

Time constants (or taus) estimated by the CRMP are also comparable to original *lt*CRMP time constants (see Figure 3.5). Figure 3.6 shows the total production match for all producers in the streak case.

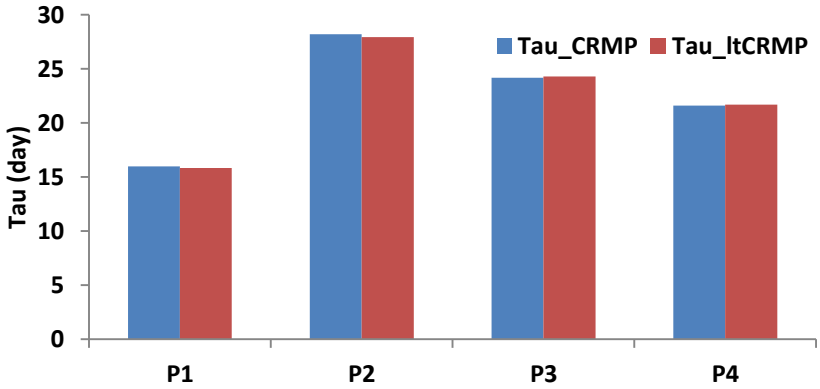

Figure 3.5: Comparison between CRMP time constants and *lt*CRMP time constants in the streak case.

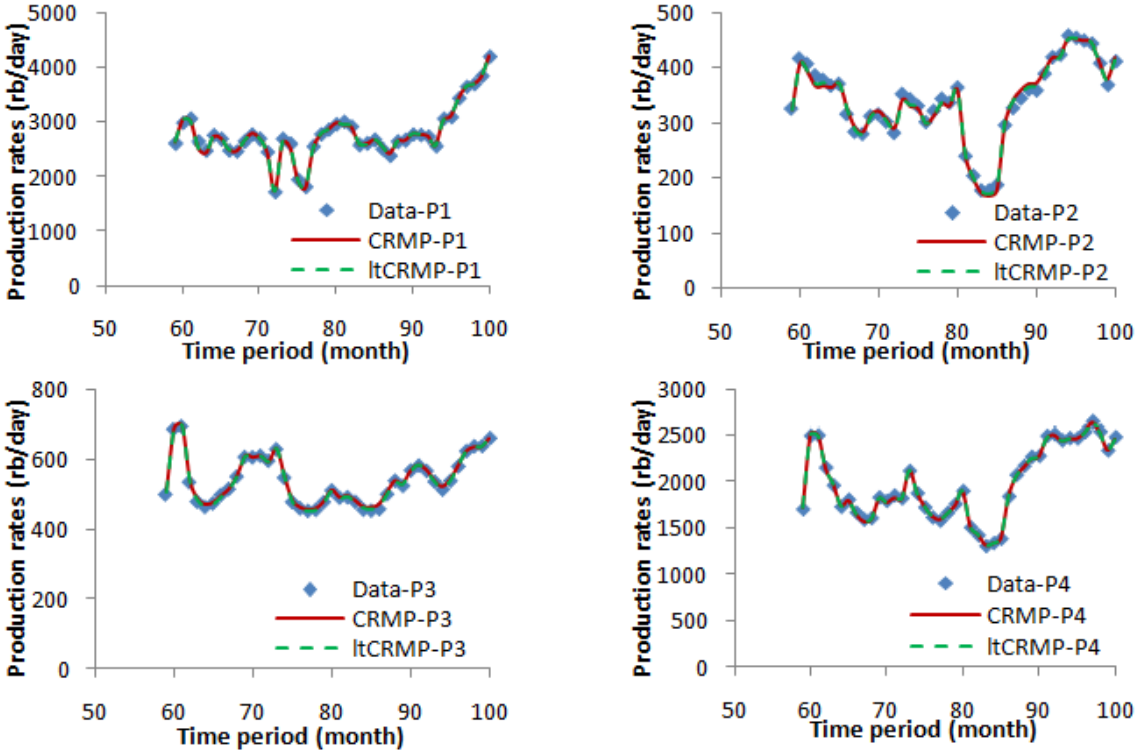

Figure 3.6: Streak case CRMP and *lt*CRMP match of total production.

The R^2 value quantifies the goodness of fit, and R^2 values for CRMP and ICRM fits for all four producers are shown in Figure 3.7. Although both CRMP and *lt*CRMP fit the data well with large R^2 value (close to one) as shown in Figure 3.7, the smaller value of the objective function resulted from the *lt*CRMP indicates that *lt*CRMP fits better than CRMP (see Figure 3.8).

In Synfield-1 we expect the majority of the water injected into I1 would flow towards P1 because there is a high-permeability (1000 md) streak between I1 and P1. The interwell connectivity calculated by both models between I1 and P1 is 0.896, the highest gain obtained. The large gain indicates 90 % of the water injected into I1 travelled to P1

(at steady state), as expected. The gain calculated by both models for another high-permeability (500 md) streak between I3 and P4 also indicates 65% of water injected into I3 travelled towards P4. Therefore, the estimated interwell connectivities obtained from both CRMP and ICRM are consistent with the imposed geology.

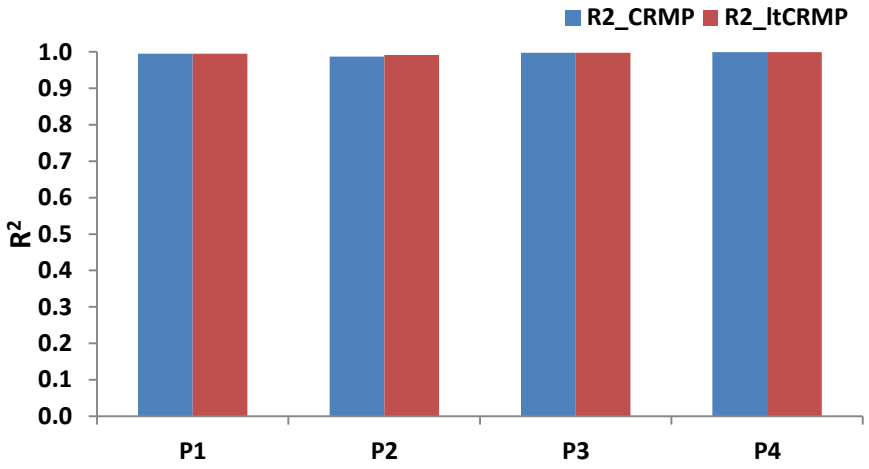

Figure 3.7: R^2 values of fits calculated by CRMP and *lt*CRMP.

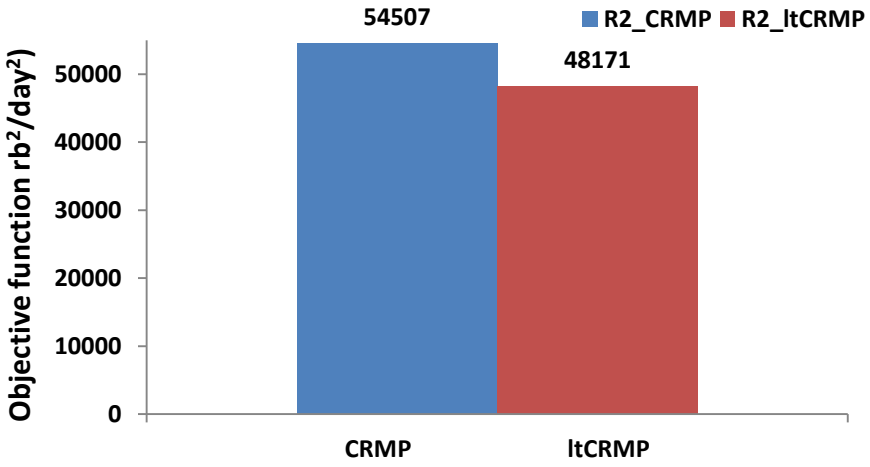

Figure 3.8: Comparison of optimal objective function between CRMP and *lt*CRMP.

If data quality is good, like those generated by simulators, one can expect to obtain good fits via regression as long as correct models are applied to fit data. When the *lt*CRMP is used to match the total production data, it is critical to plot them using the CRMP with the original *lt*CRMP parameters. If measured production rates change smoothly in a continuous fashion like the data observed from Synfield-1, then seemingly good fits can be obtained regardless of the quality of the data.

For example, Figure 3-9 shows the total production match in Synfield-1 with f'_{ij} equal to zero and e_j equal to one for all producers. These *lt*CRMP fits shown in Figure 3-9 seem acceptable, and the quality of fits is fair. However, original gains calculated by the effective gains indicate the degree of communication between all injector-producer well pairs is zero. Also, original time constants calculated from the transformed time constants are infinite numbers, indicating either Synfield-1 has infinite pore volume or the fluid is infinitely compressible. These results are not consistent at all with the assumed geology in Synfield-1. Figure 3.10 shows the CRMP fits for Synfield-1 with zero gains and infinite time constants.

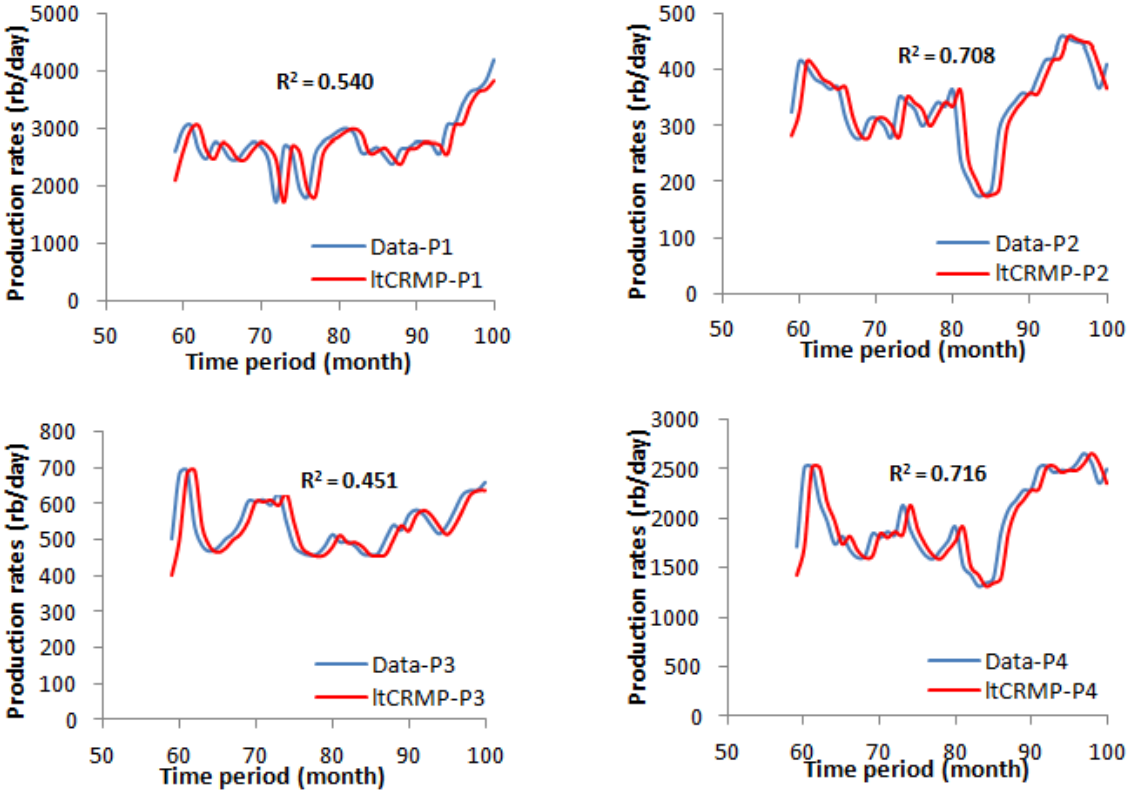

Figure 3.9: *lt*CRMP match of total productions in Synfield-1. Effective gain (f'_{ij}) is zero for all well-pairs, and e_j is one for all producers.

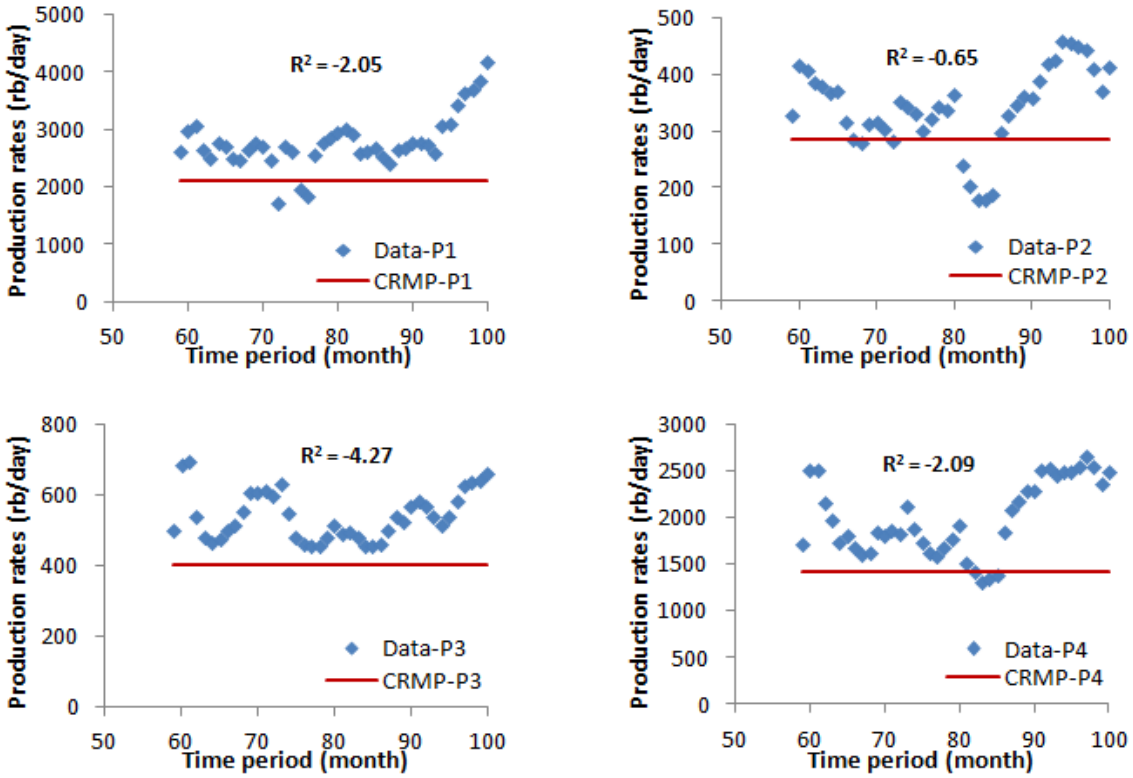

Figure 3.10: CRMP match of total productions in Synfield-1. Gain (f_{ij}) is zero for all well-pairs, and τ_j is infinite number for all producers.

If some producers with few data points or many data outliers are observed, then it would be difficult to obtain a set of model parameters that are consistent with imposed geology of the reservoir and provide good regression fits. This problem can be alleviated by maximizing the time constants (equivalent to fixing e_j to be one) when the *lt*CRMP is used to carry out history-matching. When e_j is one and f'_{ij} is zero, calculated total liquid production rate at time step k ($(q_k)_{cal}$) is observed total liquid production rate at time step k-1 ($(q_{k-1})_{obs}$), yielding a fair value of R^2. In this case, the regression fit overlaps the data if the *lt*CRMP is shifted by one time period as shown in Figure 3-11. Unfortunately, observed field production data such as both oil and water production rates often change

smoothly in a continuous fashion in real fields. Therefore, it is suggested to re-plot the CRMP with the original model parameters that are calculated from the *lt*CRMP parameters when the quality of production data is obviously poor.

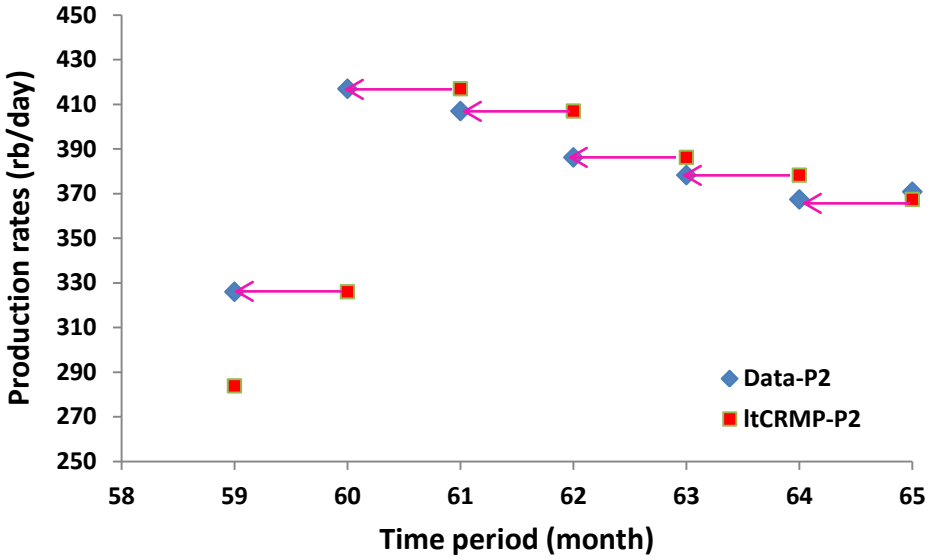

Figure 3.11: CRMP match of total productions for P2 in Synfield-1. f'_{i2} is zero, and e_2 is one.

3.1.2 CRMP vs. ICRM

Prior to comparing the two models (CRMP and ICRM), the sensitivity of the ICRM parameters to relaxing the constraints was examined for the balanced waterflood. The ICRM was applied to match simulated data starting from month 58 to month 100, and the model parameters were estimated by both the unconstrained LMR and the constrained LMR. The results show (see Table 3.4) that the model parameters estimated by the both regression methods are essentially the same, confirming the ICRM

parameters are insensitive to relaxing the constraints for the balanced waterflood (Synfield-1). When the constraint (Equations 2.9) was ignored in ICRM optimization, the sum of the gains over all producer indices for I1, I2, and I4 was slightly greater than one, violating the material-balance requirements. However, these values are sufficiently close to ones to effectively satisfy the material-balance requirements in a waterflooded reservoir.

Table 3.4: Inferred ICRM parameters for the streak case

Unconstrained NMR / Constrained NMR		**I1**	**I2**	**I3**	**I4**	**I5**	τ_i **(day)**
P1	Unconstrained f_{i1}	0.8961	0.5926	0.1981	0.2515	0.1625	5.16
	Constrained f_{i1}	0.8935	0.5907	0.2013	0.2397	0.1739	5.16
P2	Unconstrained f_{i2}	0.0357	0.0351	0.0402	0.2047	0.0330	13.64
	Constrained f_{i2}	0.0332	0.0332	0.0434	0.1928	0.0444	13.64
P3	Unconstrained f_{i3}	0.0199	0.1808	0.0856	0.0400	0.1660	12.27
	Constrained f_{i3}	0.0173	0.1789	0.0888	0.0282	0.1774	12.27
P4	Unconstrained f_{i4}	0.0586	0.1992	0.6634	0.5511	0.5929	10.60
	Constrained f_{i4}	0.0560	0.1973	0.6666	0.5393	0.6043	10.60
$\sum_{j=1}^{n_p} f_{ij}$	Unconstrained	1.010	1.008	0.987	1.047	0.954	
	Constrained	1.000	1.000	1.000	1.000	1.000	

Figure 3.12 shows the comparison between CRMP gains estimated by the constrained NMR and ICRM gains estimated by the LMR presented in histograms. The results show the gains estimated from the both models are comparable to each other. The

estimated interwell connectivities obtained from ICRM are consistent with the imposed geology.

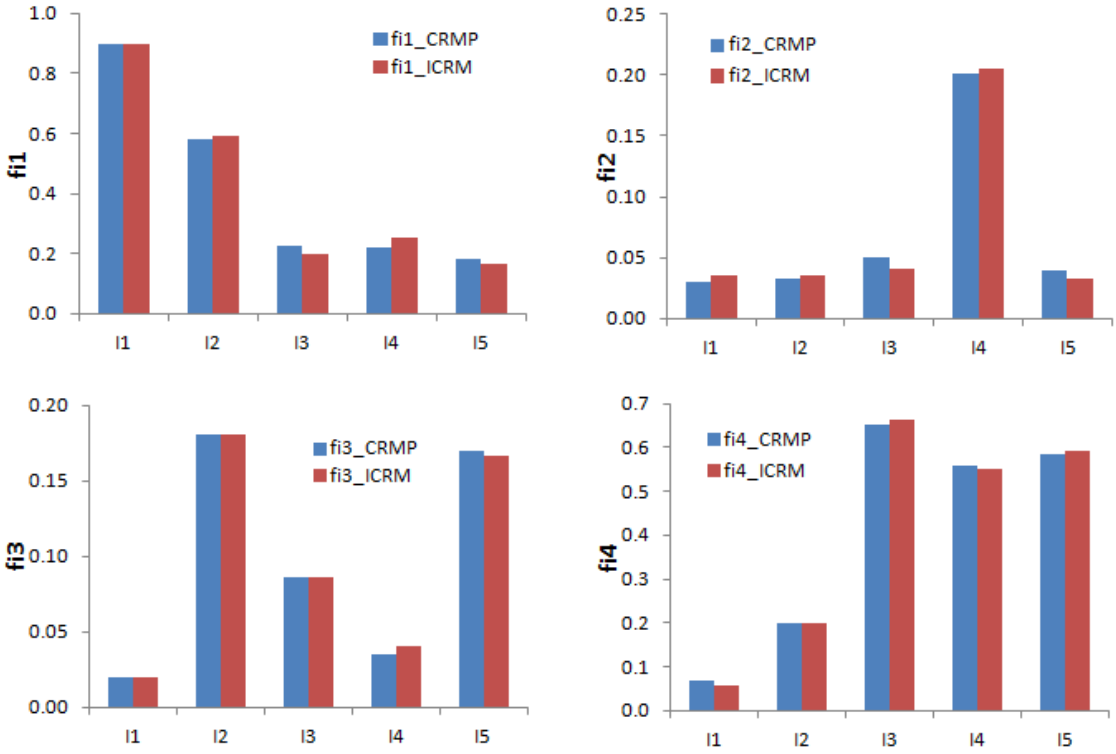

Figure 3.12: Comparison between CRMP gains and ICRM gains for P1, P2, P3, and P4 in the streak case. Subscript i is an injector index in the range 1 to 5.

Time constants (or taus) estimated by the CRMP are about twice those estimated by the ICRM, but the two quantities are of the same order of magnitude (see Figure 3.13). The cause of this bias is that the observed cumulative production has been overestimated. The ICRM fit could be improved by decreasing the time constant when the model is fitted on overestimated responses (cumulative production). Figure 3.14 shows the total production match for all producers in the streak case. R^2 values for CRMP and ICRM fits for all four producers are shown in Figure 3.15.

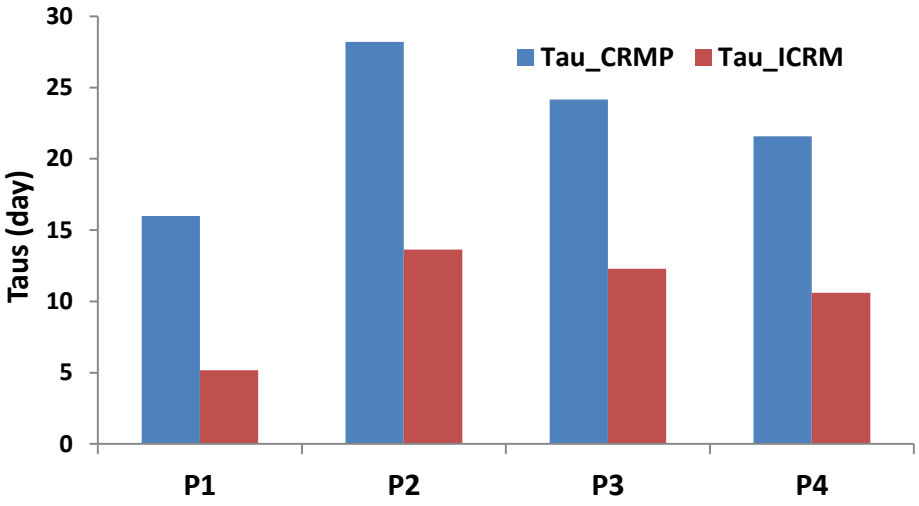

Figure 3.13: Comparison between CRMP time constants and ICRM time constants in the streak case.

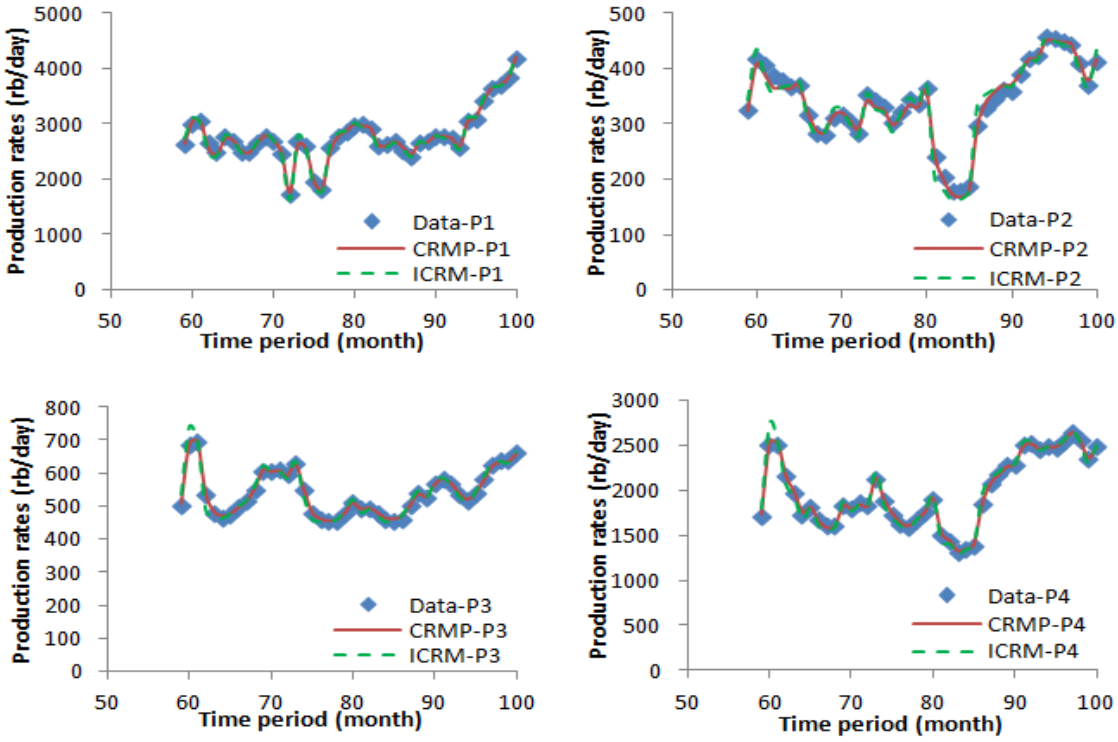

Figure 3.14: Streak case CRMP and ICRM match of total productions.

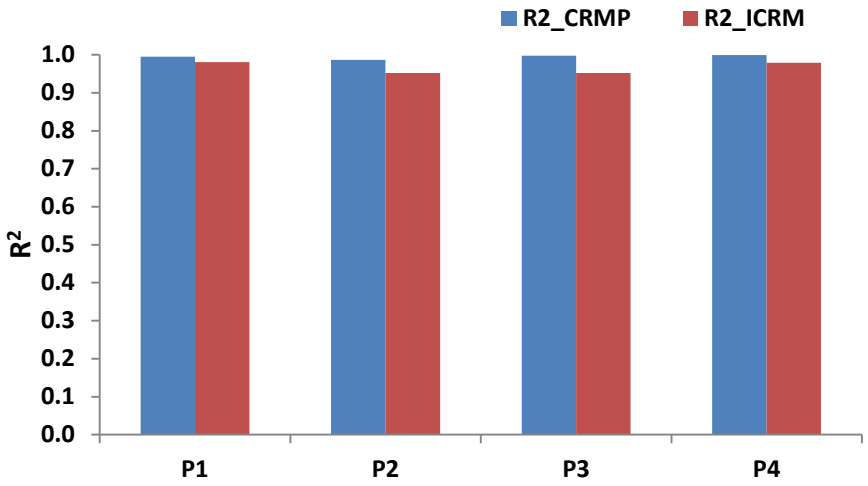

Figure 3.15: R^2 values of fits calculated by both CRMP and ICRM.

3.2 Synfield-2: Complete Sealing Barrier

Like a case of Synfield-1, Synfield-2 consists of five vertical injectors and four vertical producers. Figure 4.16 shows the location of wells and sealing barriers of Synfield-2. This field is characterized as a homogeneous isotropic reservoir with porosity of 20% and permeability of 50 md. However, this field is divided into three by a sealing fault. Table 4.5 provides the average reservoir and fluid properties.

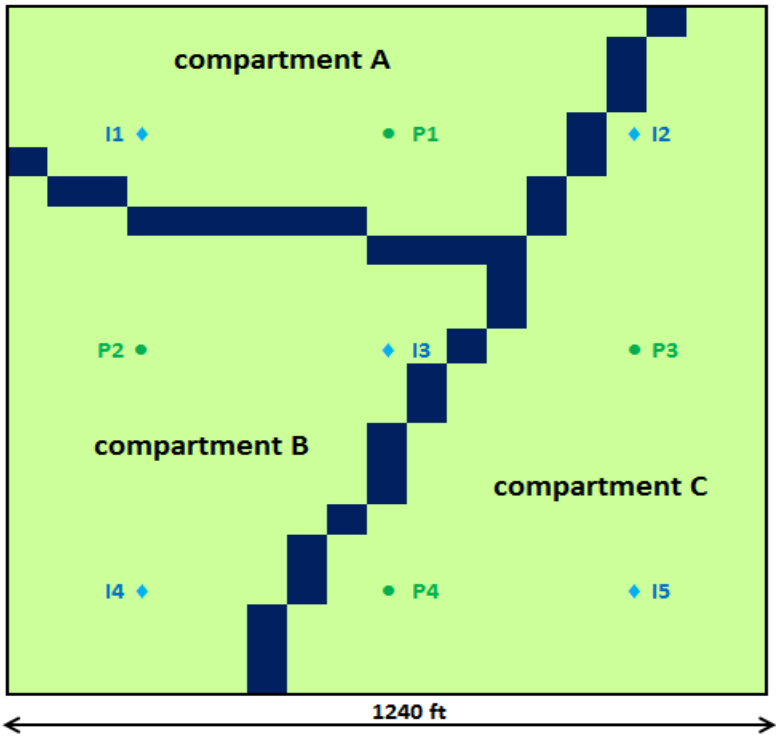

Figure 3.16: Synfield-2 is a homogeneous isotropic reservoir (k=50 md and ϕ=0.2) and consists of three compartments that do not communicate with each other because of the presence of fault seals.

Table 3.5: Average reservoir and fluid properties of Synfield-2

Size (ft^3)	1240 × 1240 × 200
Number of grid blocks	33 × 33 × 5
Permeability (md)	50
Porosity (%)	20
Initial reservoir pressure (psi)	1250
Initial water saturation	0.3
Producer bottom-hole pressure constraint (psi)	250
Depth of a top layer from the surface (ft)	1600

All four producers started in January 2005, and water was injected into all five injectors from January 2006 until the end of the simulation, January 2015. Historical

water injection rates used in Synfield-2 were the same as those used in Synfield-1 (Figure 3.2). The producer BHPs were kept constant at 250 psi during the simulation, and a constrained linear regression was done using the ICRM to match the IMEX simulated cumulative production starting from January 2007 to November 2010. Simulated total production rates for Synfield-2 are shown in Figure 3.17. Table 3.6 shows the estimated parameters from the ICRM in Synfield-2.

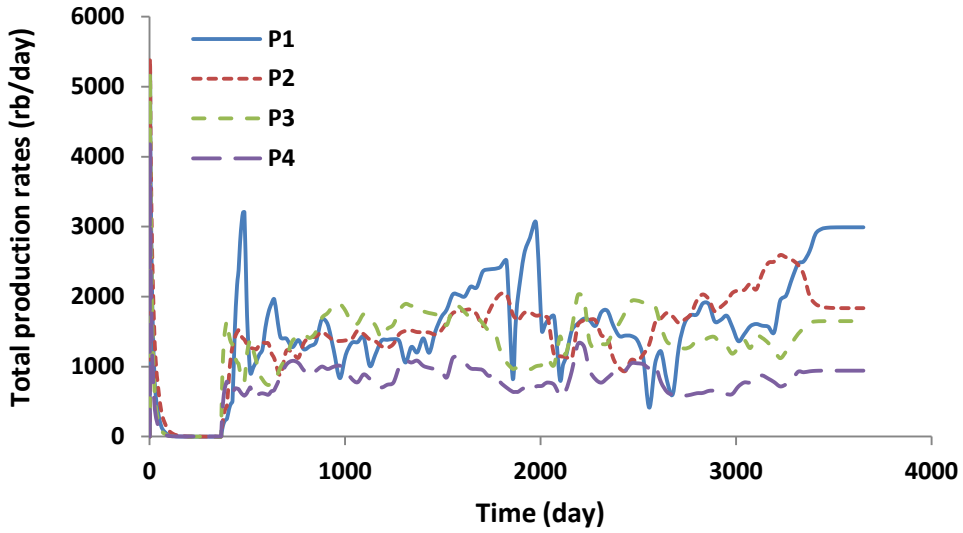

Figure 3.17: Monthly total liquid production rates of four producers in Synfield-2.

Table 3.6: Inferred ICRM parameters for Synfield-2

f_{ij}	I1	I2	I3	I4	I5	τ_j (day)
P1	1.0000	0.0000	0.0000	0.0000	0.0000	8.359
P2	0.0000	0.0000	0.9995	1.0000	0.0000	33.04
P3	0.0000	0.7461	0.0001	0.0000	0.5002	25.98
P4	0.0000	0.2539	0.0005	0.0000	0.4996	22.89

In compartment A, there is one injector, I1, and one producer, P1; therefore, we expect I1 to only communicate with P1. The estimated gain between I1 and P1 is truly one, indicating all the water injected into I1 travelled only to P1. This result agrees exactly with the imposed geological information.

Compartment B contains two injectors, I3 and I4, and one producer, P2. The estimated gains of the I3/P2 and I4/P2 well-pairs are 0.9995 and 1.These results suggest that there are no-flow boundaries around I3, I4, and P2 and that these wells are isolated from the rest of wells in this field.

In compartment C, I5 is an equal distance from producers P3 and P4, so we can expect water injected into I5 to be equally distributed to P3 and P4. The result shows that half the water injected into I5 travelled to P3 (0.5002) and that the other half travelled to P4 (0.4996). There is another injector, I2, in compartment C, and the distance of I2/P4 well-pair is 2.25 times greater than that of I2/P3 well-pair. The interwell connectivities of I2/P4 and I2/P3 well-pairs are 0.2539 and 0.7461, respectively, and these results are consistent with the larger connectivities encountered for close injector-producer well-pairs (Sayarpour, 2008).

When injectors fall in one compartment, and producers fall in another, there should be no communication between injector-producer well-pairs, and estimated gains of these well-pairs are zero as expected. The total production match of all producers for Synfield-2 is shown in Figure 3.18. The ICRM results fit the data well.

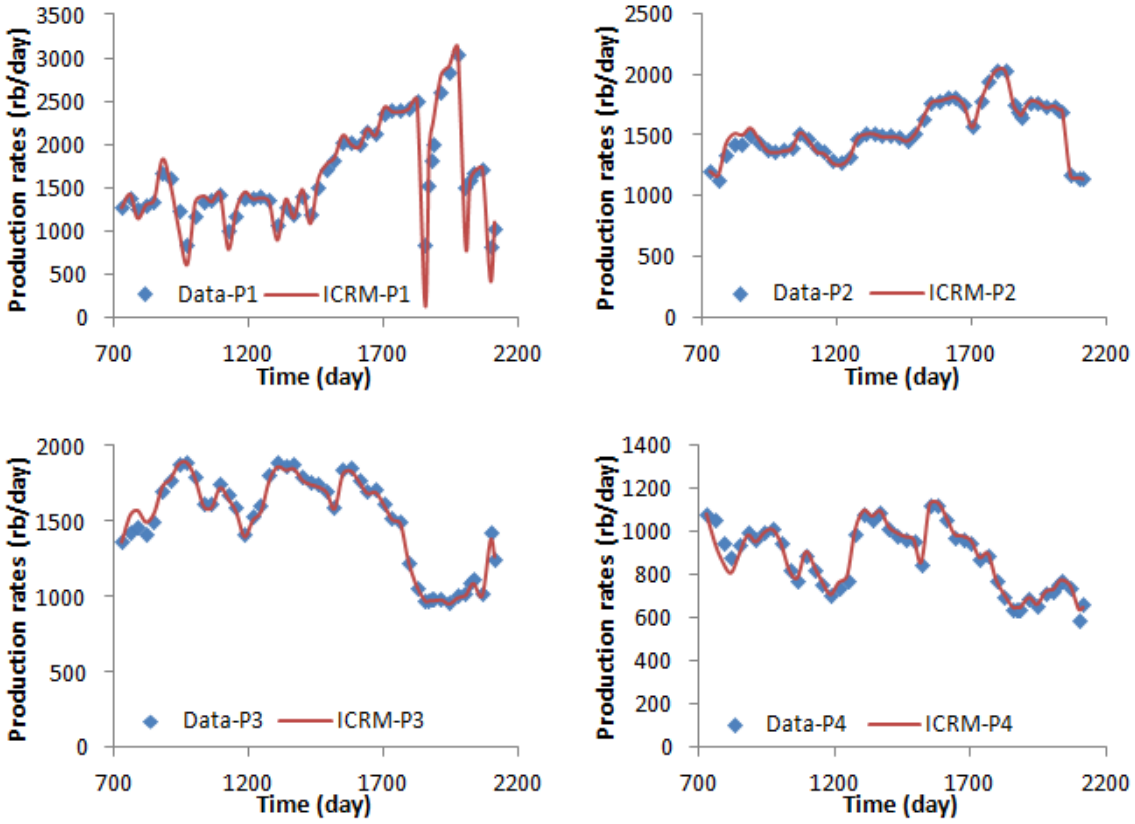

Figure 3.18: ICRM match of total production in Synfield-2.

3.3 Synfield-3: Partially Sealing Barrier

Synfield-3 is identical to Synfield-2 except the barrier is only partially sealing. Constrained linear regression was done using the ICRM to match the IMEX simulated cumulative production starting from January 2007 to November 2010. Table 3.7 shows the estimated parameters from the ICRM in Synfield-3. Figure 3.19 shows the location of wells and sealing barriers of Synfield-3.

Table 3.7: Inferred ICRM parameters for Synfield-3

f_{ij}	I1	I2	I3	I4	I5	τ_j (day)
P1	0.0326	0.4670	0.0409	0.0827	0.1257	27.79
P2	0.6286	0.0737	0.3560	0.4568	0.1410	13.84
P3	0.1000	0.3550	0.1717	0.1470	0.3659	13.45
P4	0.2388	0.1043	0.4314	0.3135	0.3674	13.40

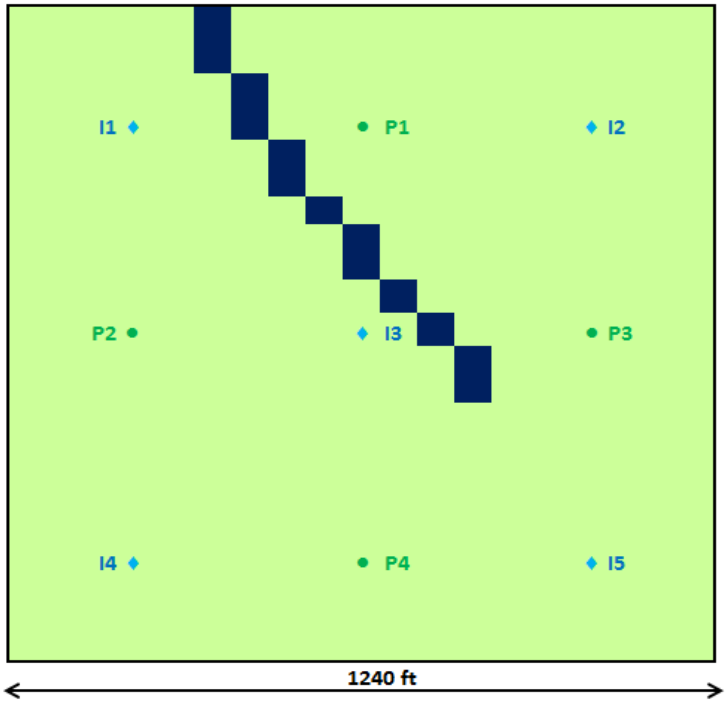

Figure 3.19: Synfield-3 is a homogeneous isotropic reservoir (k=50 md and ϕ=0.2) with a partially sealing barrier (blue diagonal blocks).

The result shows that the presence of transmissibility barrier can be inferred by interwell connectivities (*gains*) estimated by the ICRM. Low interwell connectivities are found for injector-producer well-pairs on each side of the barrier and close to the barrier.

For example, the estimated gains of the I1/P1 and I3/P1 well-pairs are 0.0326 and 0.0409, and these results suggest that there is a transmissibility barrier (or no-flow boundary) between P1 and injectors I1 and I3. The total production match of all producers for Synfield-3 is shown in Figure 3.20.

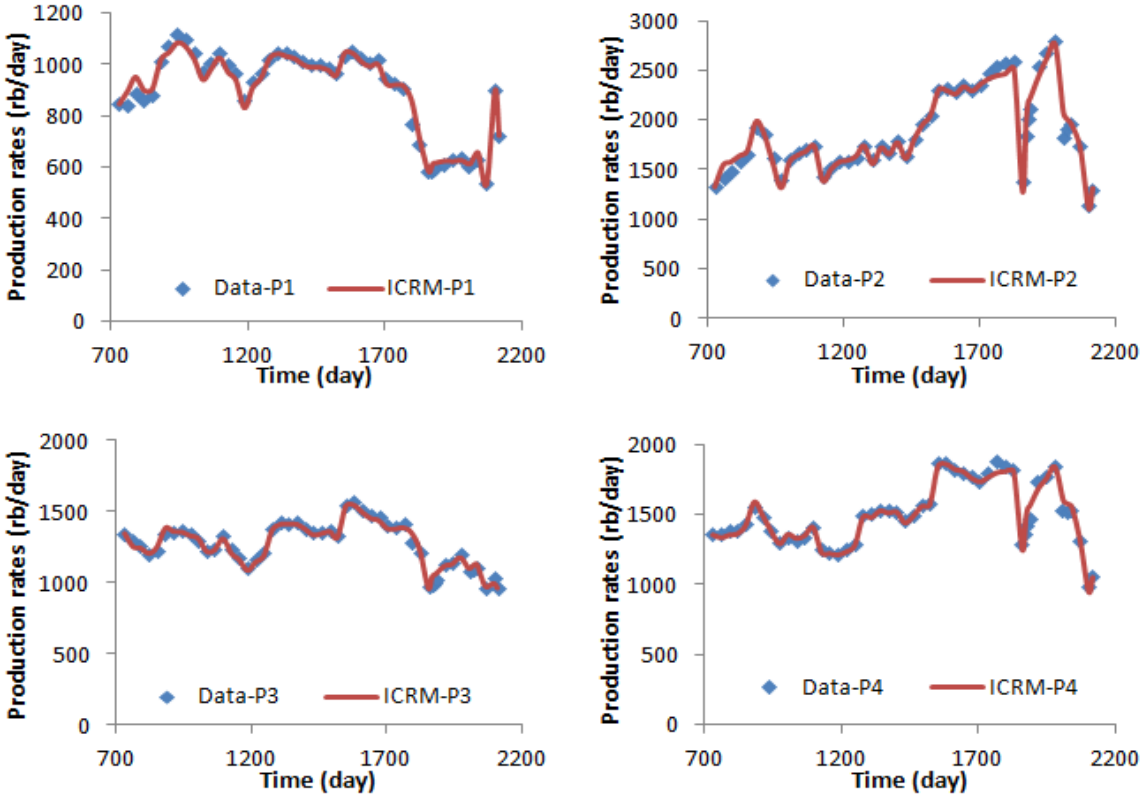

Figure 3.20: ICRM match of total productions in Synfield-3.

3.4 Synfield-4: Wells in Random Locations

The relationship between interwell-connectivity and interwell-distance is studied by applying simple reservoir models on Synfield-4. This synthetic reservoir is

characterized as a homogeneous isotropic reservoir where wells (five water injectors and four producers) are located randomly (see Figure 3.21).

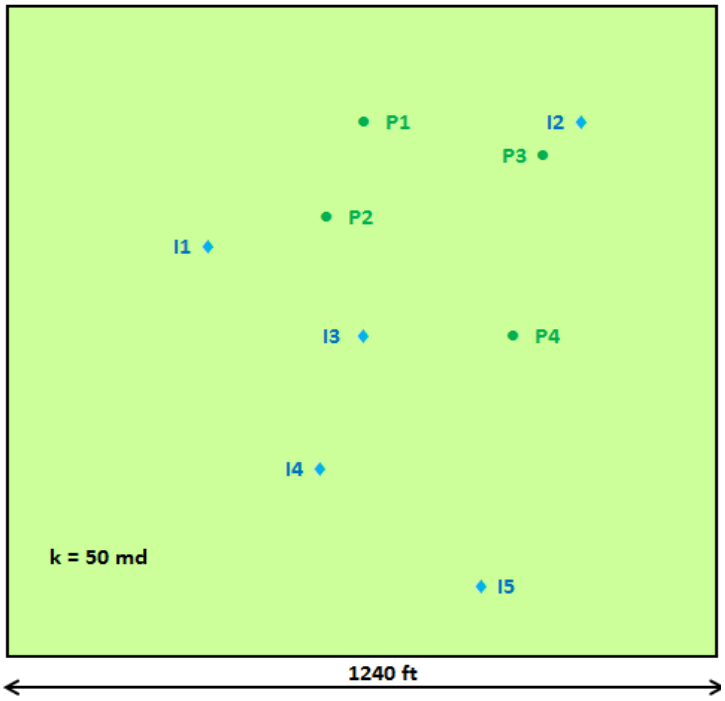

Figure 3.21: Synfield-4 is a homogeneous isotropic reservoir (k=50 md and ϕ=0.2) and consists of five water injectors and four producers.

Both CRMP and ICRM were applied to match simulated data starting from January, 2007 to November, 2010. The CRMP parameters were estimated via constrained NMR, and the ICRM parameters were estimated via constrained LMR. The CRMP and ICRM parameters are shown in Figures 3.22 and 3.23. The results show model parameters estimated from the both models are comparable to each other. Figure 3.24 shows the total production match for all producers in Synfield-4.

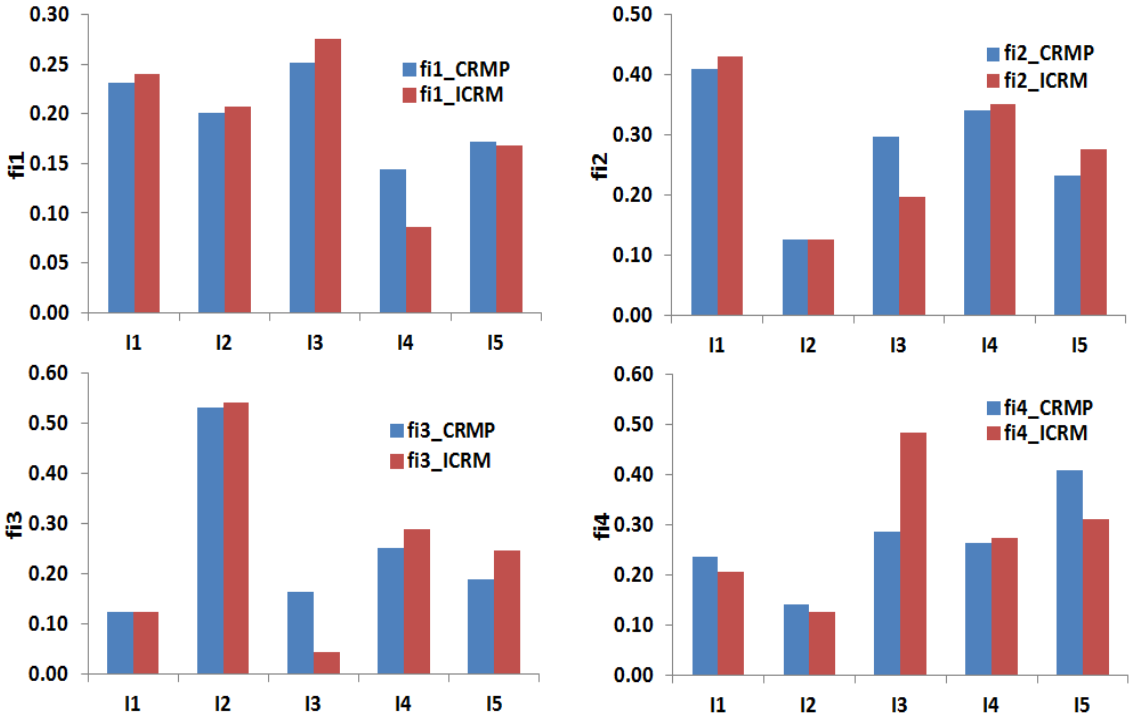

Figure 3.22: Comparison between CRMP gains and ICRM gains for P1, P2, P3, and P4 in Synfield-4. Subscript i is an injector index in the range 1 to 5.

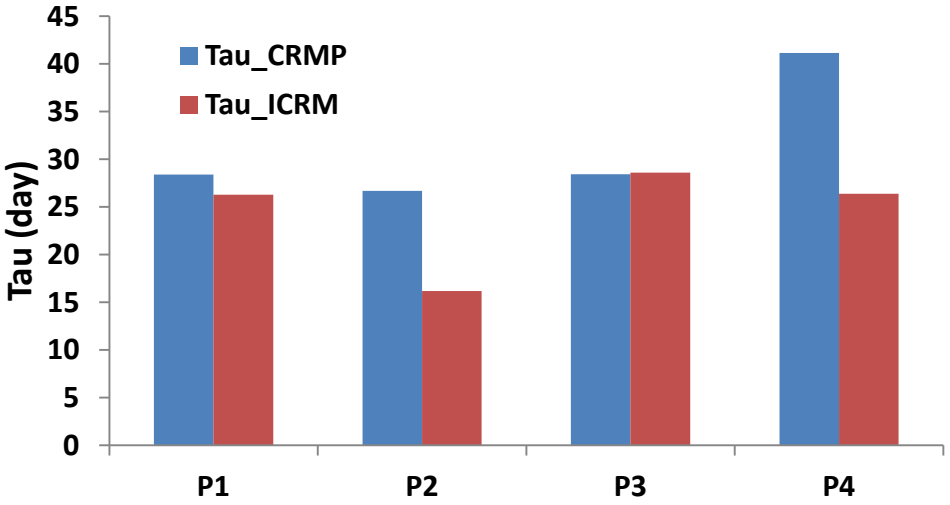

Figure 3.23: Comparison between CRMP time constants and ICRM time constants in Synfield-4.

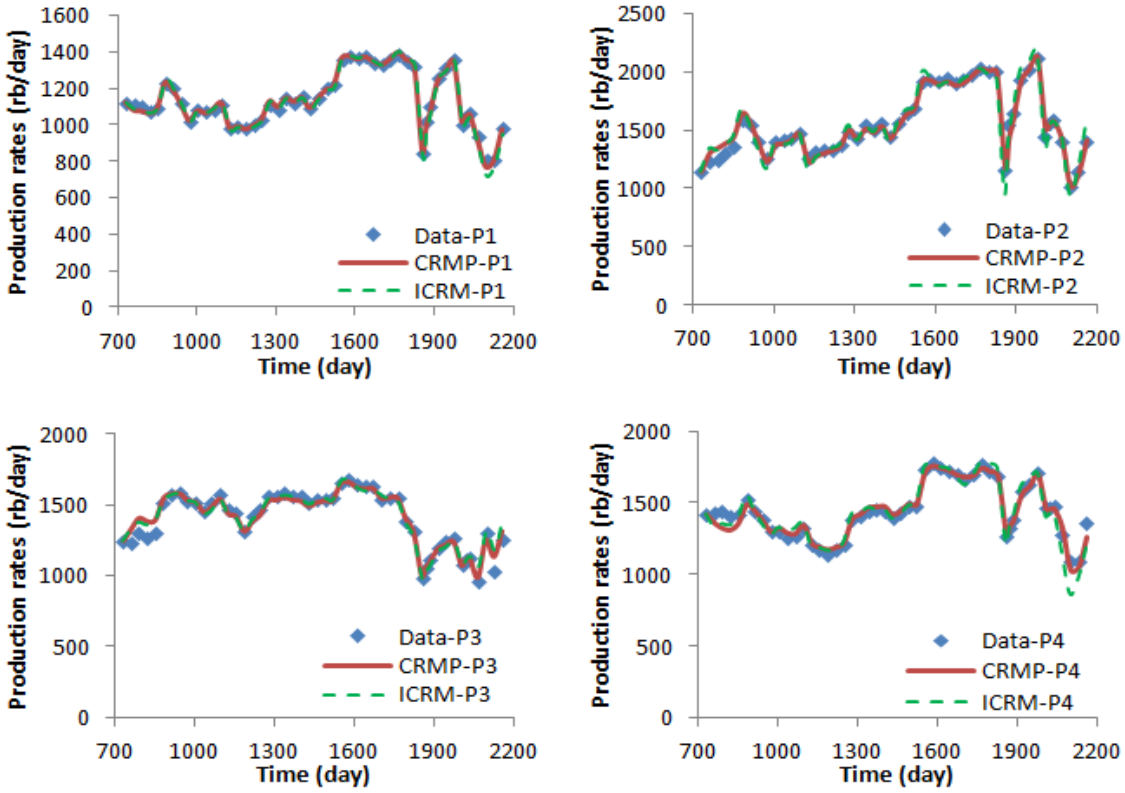

Figure 3.24: Synfield-4 CRMP and ICRM match of total productions.

If the relationship between the gain and the interwell-distance between injector-producer well-pair is assumed to be linear, one can estimate an interwell-distance dependent gain (f_{ij}^{d}) at a given interwell-distance:

$$f_{ij}^{d} = Ad_{ij} + B \qquad (3.1)$$

where d_{ij} is an interwell-distance between injector-producer well-pair, and A and B are fitting parameters. Fitting parameters (A and B) can be estimated by regressing Equation 3.1 on ICRM gains. Equation 3.1 should only be used to interpolate gains; therefore, it is valid in the range of $f_{ij,lo}$ to $f_{ij,hi}$, where $f_{ij,lo}$ is the lowest gain and $f_{ij,hi}$ is the highest gain estimated for a given reservoir.

In Figure 3.25, ICRM *gains* estimated from Synfield-4 are plotted on the y-axis and the corresponding well-distance between each injector-producer pair is plotted on the x-axis. As expected, the well-connectivity (gain) tends to decrease as the interwell-distance increases. Equation 3.1 was linearly regressed on ICRM gains in Synfield-4, and regression coefficients were found to be -0.0003 ft^{-1} for *A* and 0.401 ft for *B*.

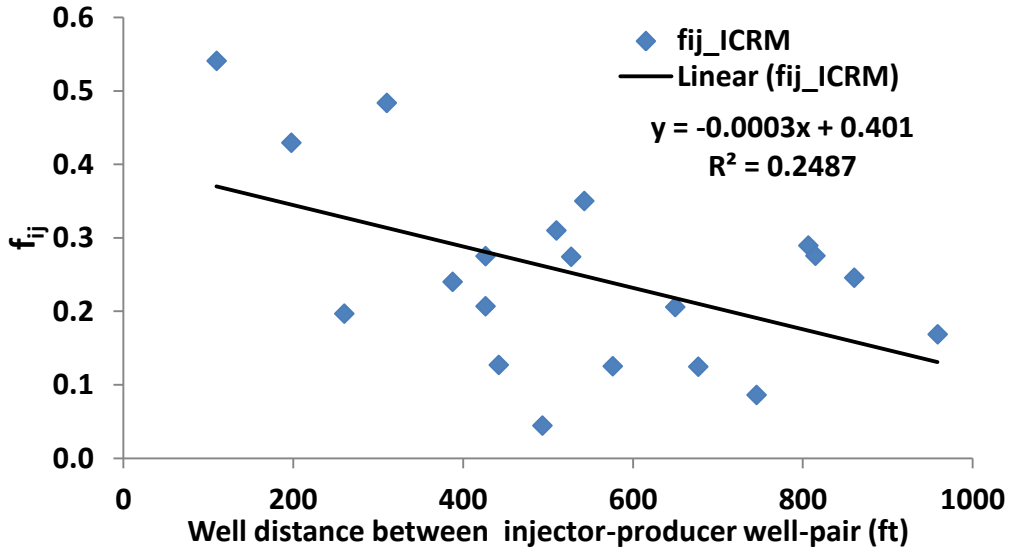

Figure 3.25: ICRM gain vs interwell-distance (d_{ij}) in Synfield-4.

In Table 3.8, the *gain* calculated by Equation 3.1 (f_{ij}^{d}) is compared to the ICRM gain (f_{ij}) with corresponding d_{ij} for Synfield-4.

Table 3.8: Comparison between f_{ij} and f_{ij}^{d} for Synfield-4

d_{ij} (ft)	f_{ij}	f_{ij}^{d}
110	0.5409	0.3681
198	0.4294	0.3417
260	0.1968	0.3230
310	0.4837	0.3080
388	0.2401	0.2848
426	0.2068	0.2731
426	0.2751	0.2731
442	0.1270	0.2685
493	0.0444	0.2530
510	0.3100	0.2481
527	0.2742	0.2429
543	0.3502	0.2383
576	0.1253	0.2282
650	0.2059	0.2061
677	0.1246	0.1980
745	0.0861	0.1774
806	0.2895	0.1591
815	0.2756	0.1566
860	0.2457	0.1429
959	0.1687	0.1134

Although R^2 values of the fits based on f_{ij}^{d} are not as good as R^2 values of ICRM fits (see Figure 3.26), these fits are able to capture the general trends of the reservoir production observed in Syfield-4 as shown in Figure 3.27.

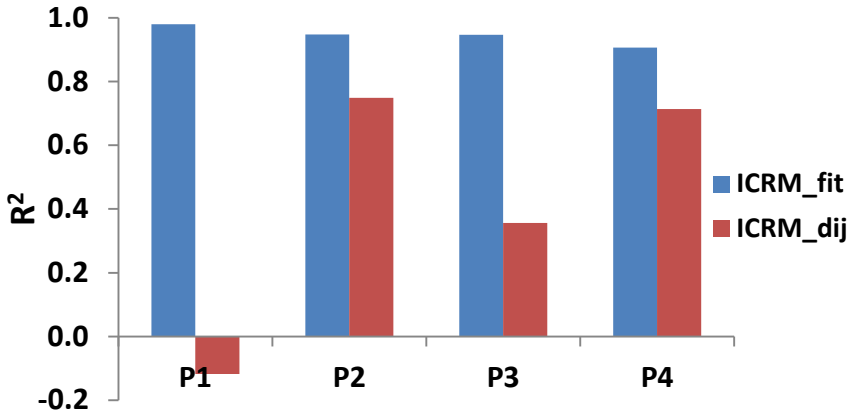

Figure 3.26: R^2 values of ICRM fits (blue histograms) and the fits based on f_{ij}^{d} (red histograms) for Synfield-4.

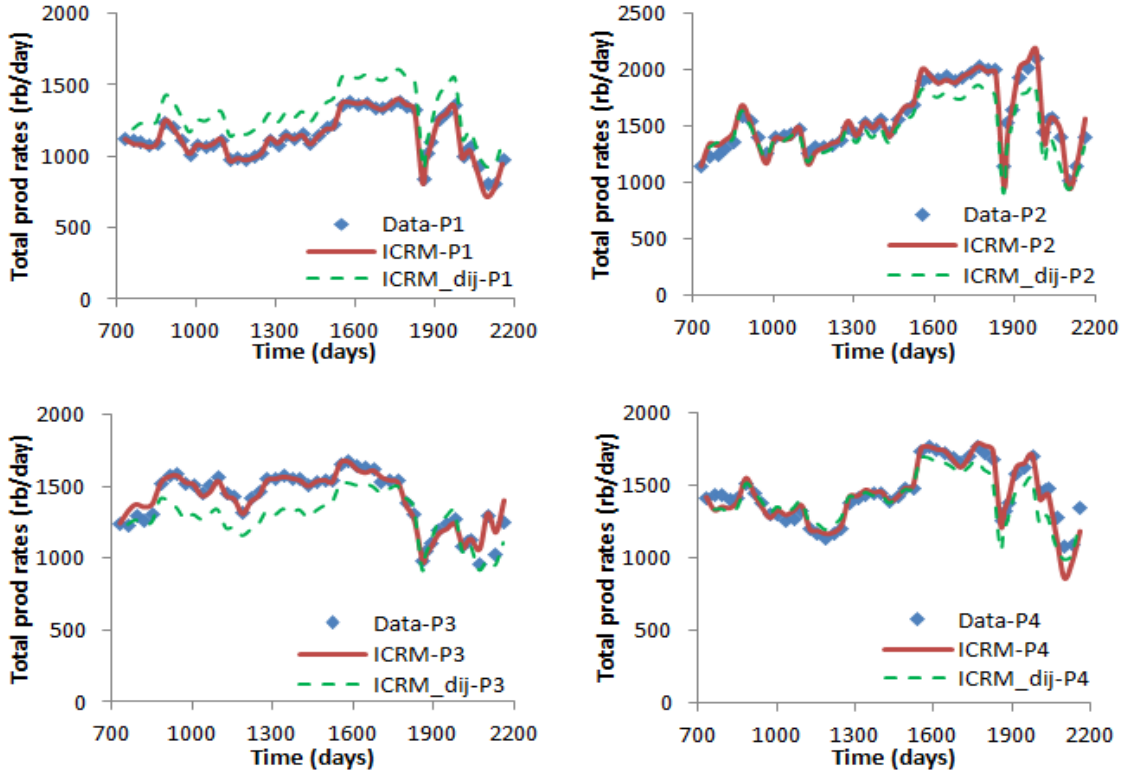

Figure 3.27: ICRM fits (red solid line) and predicted total production rates based on f_{ij}^{d} (green dashed line) for Synfield-4.

3.5 Synfield-5: Wells in Random Locations with New Injectors

The allocation factor for water injection rate can be estimated reasonably from the interwell-distance between well-pairs. This allows approximation of well-connectivities between newly drilled injectors and existing producers in homogenous reservoirs. Synfield-5 (Figure 3.28) is identical to Synfield-4, but two injection wells (I6 and I7) were added in a reservoir after 2200 days (six years) of oil production. After new injectors have been added in a reservoir, oil production has been carried out for an additional four years.

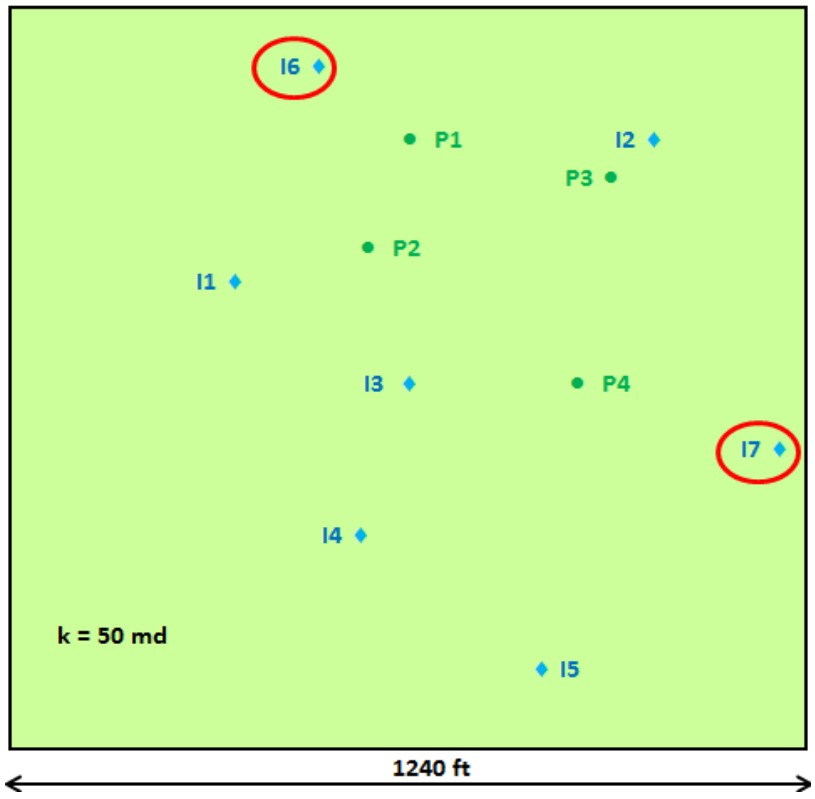

Figure 3.28: Synfield-5 is a homogeneous isotropic reservoir (k=50 md and ϕ=0.2) and consists of five water injectors and four producers initially. After six years of oil production, two injectors (I6 and I7) have been added in the reservoir.

In Figure 3.29, adding two new injectors supported reservoir pressure substantially, causing a sudden increase in total production rates of all four producers after oil production has occurred for 2200 days.

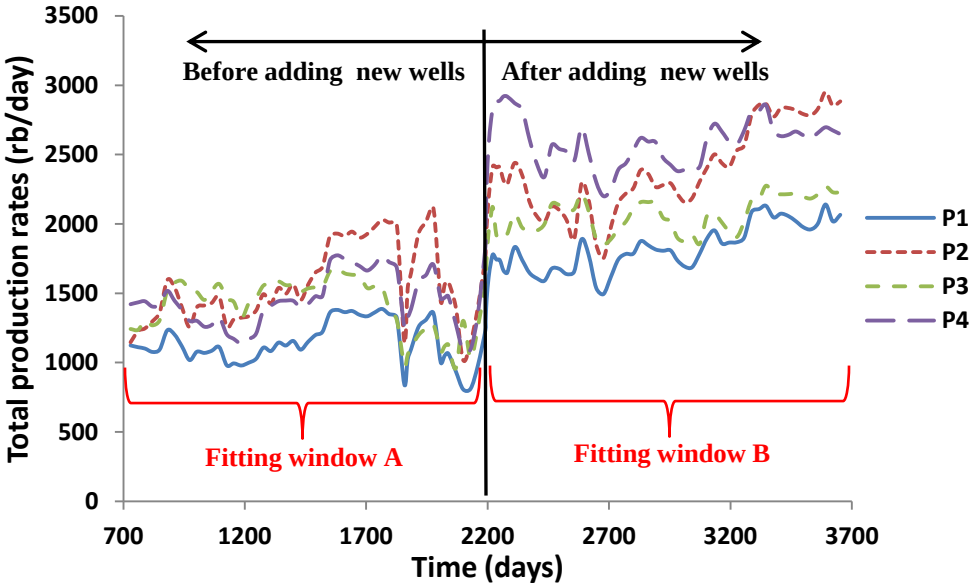

Figure 3.29: Daily total liquid production rates of four producers in Synfield-5.

Predicting gains between newly added injectors and producers by using Equation 3.1 would make sense only if it is assumed that the model parameters remain constant with the introduction of new injectors. To validate this assumption that model parameters are invariant to adding new injectors, ICRM was applied on Synfield-5 by selecting two different fitting windows (see Figure 3.29). In Figure 3.30, the results show that the gains between existing injectors and producers before adding new wells do not vary significantly compared to the gains between the same well-pairs that were calculated after adding injectors.

However, the time constants decreased by about half of their original values that were estimated before adding new injectors in Synfield-5 as shown in Figure 3.31. The time constant in both CRMP and ICRM is proportional to the reservoir pore volume (V_P) and the total compressibility of the reservoir (c_t) by definition (Equation 2.4). Despite the fact that both the water and oil are considered to be relatively incompressible fluids in a black-oil reservoir, the compressibility of water is smaller than that of oil. Therefore, as more water (less compressible fluid) from newly installed injectors (I6 and I7) was injected into Synfield-5 to displace oil (more compressible fluid), the fluids in this reservoir became less compressible. Also, the contraction of the reservoir pore volume as oil production has been carried out for an additional four years was another reason for having the smaller time constants from Synfield-5 than the time constants from Synfield-4. This bias was noticeable in Synfield-5, which is a small reservoir. In real oil fields, the size of reservoirs are much larger than the size of the synthetic fields (1240 ft × 1240 ft × 200 ft) we studied, so the change in time constants to adding new injectors is expected to be less significant.

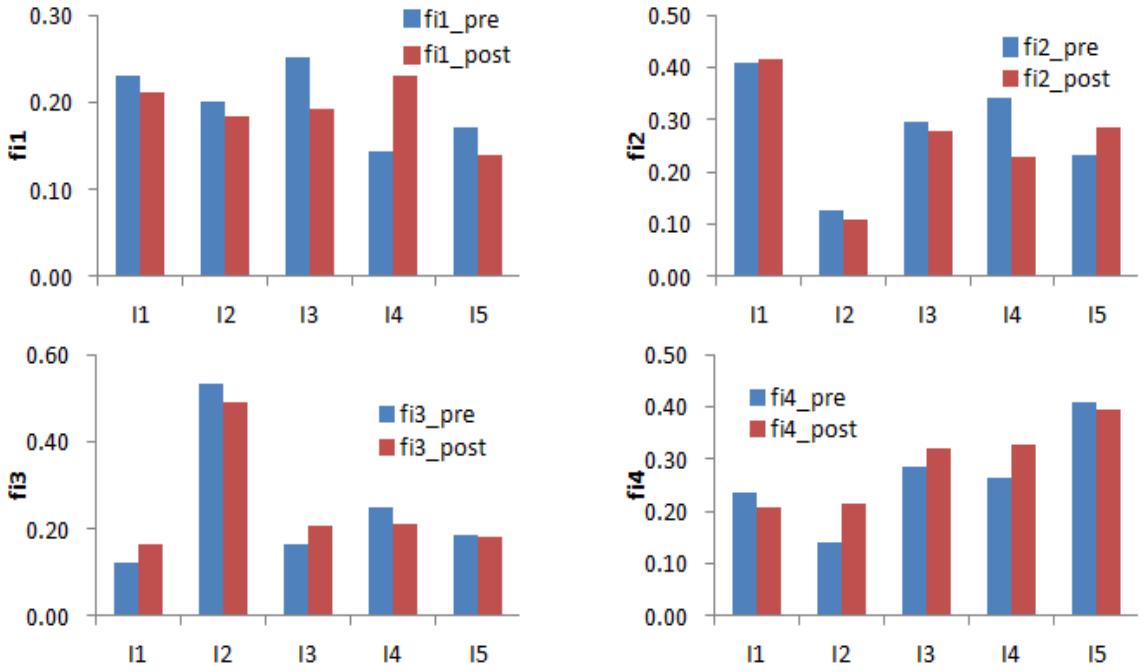

Figure 3.30: ICRM gains before adding injectors (blue histograms) vs. ICRM gains after adding injectors (red histograms) for Syfield-5. Subscript i is an injector index in the range 1 to 5.

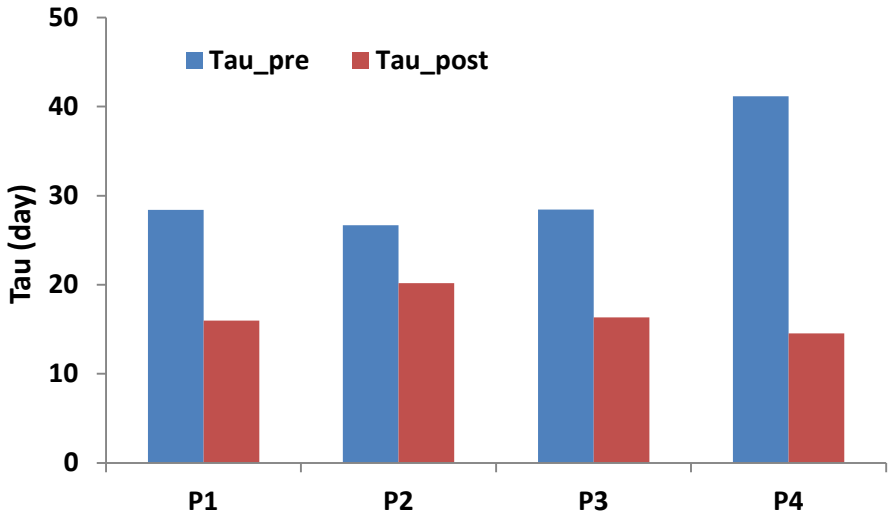

Figure 3.31: ICRM time constants before adding injectors (blue histograms) and ICRM time constants after adding injectors (red histograms) for Syfield-5.

After determining that ICRM gains between existing injectors and producers are insensitive to adding new injectors, the gains between newly added injector (I6 and I7) and producers (P1-P4) were calculated by Equation 3.1. ICRM gains were also estimated via linear regression on newly simulated data after adding two injectors. Figure 3.32 compares f_{ij}^{d} to f_{ij} and the results show that they are similar to each other (less than 30% error). These predicted gains by Equation 3.1 did not match exactly the ICRM gains but the general trend of the gains leads to an approximate solution. Furthermore, this simple approach can be used to guide reservoir simulation.

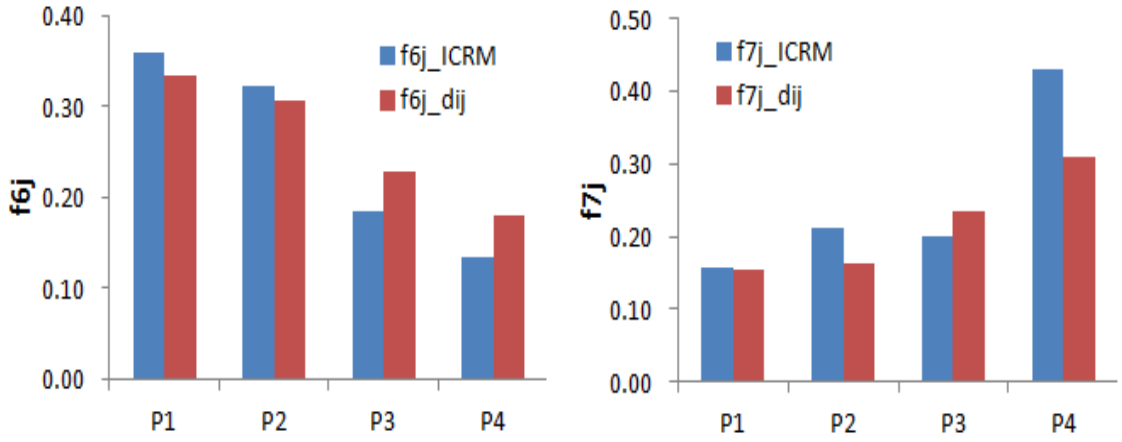

Figure 3.32: f_{ij} (blue histogram) vs. f_{ij}^{d} (red histogram) with new injectors for Synfield-5.

Finally, interwell-distance dependent gains were used to predict the future liquid productions if two injectors would have been added with known water injection scheme. In Figure 3.33, green dashed lines represent the future liquid production rates that were predicted by f_{ij}^{d} if I6 and I7 have been added in Synfield-5 after 2200 days of oil production. In the same figure, red solid lines represent the future liquid production rates

without adding new injectors. It seems that the ICRM fits based on f_{ij}^{d} are able to predict the future liquid production rates quite well if new injectors are added in the reservoir. In Figure 3.33a, it is clearly shown that the total production rates would increase substantially by Δq after 2200 days of oil production due to the additional pressure support caused by adding two new injectors.

One needs to be aware that Equation 3.1 should be used to estimate gains between new injectors and existing producers only. It should not be used to estimate gains between existing injectors and new producers. If new producers are added in a reservoir, the gains between existing injectors and producers that are calculated by regression prior to adding wells will change significantly. Also, Equation 3.1 should only be used for homogeneous reservoirs.

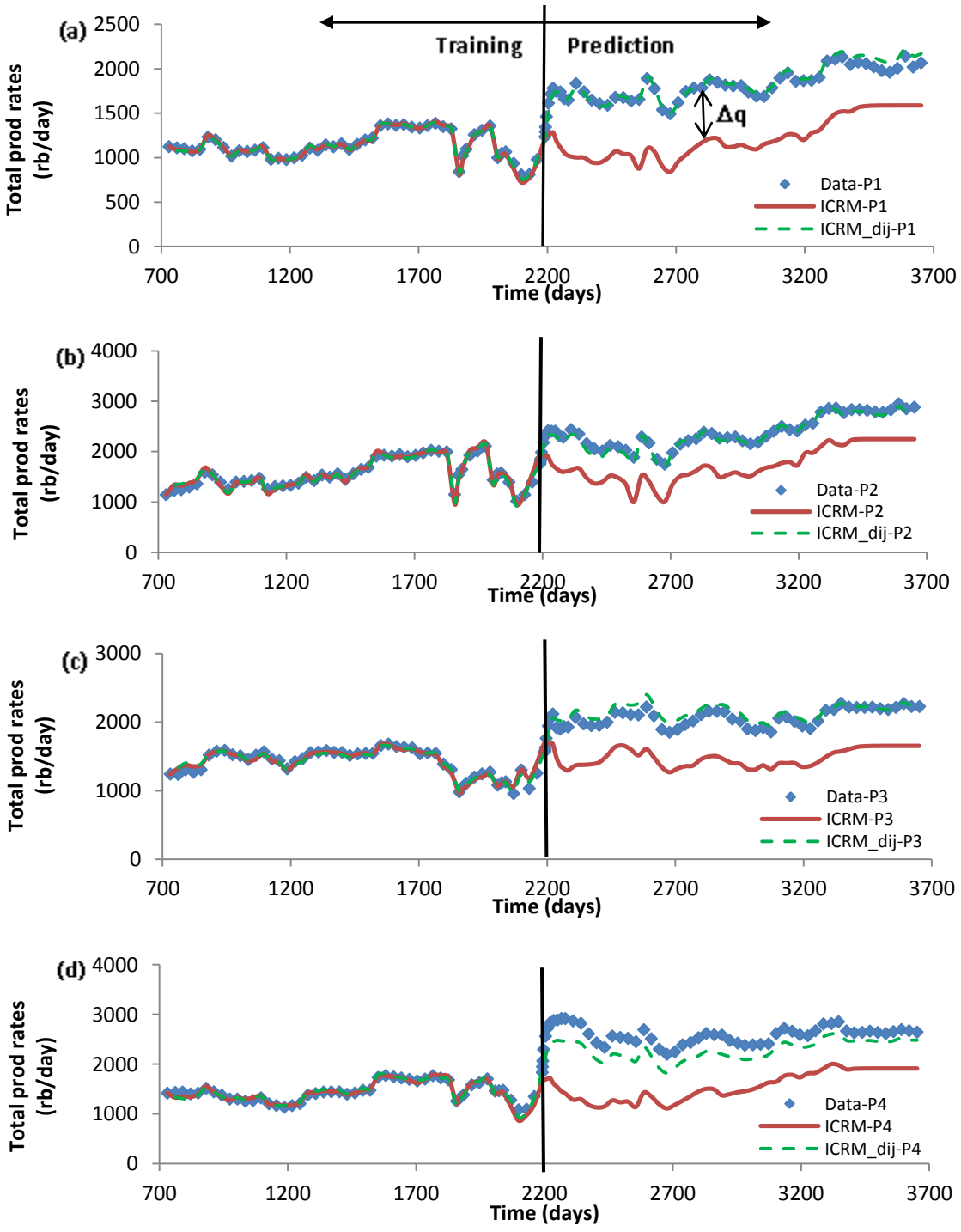

Figure 3.33: Predictions of the future total liquid production rates without (red solid line) or with new injectors (green dashed line) in Synfield-5: (a) P1, (b) P2, (c) P3, (d) P4

3.6 Summary

In this chapter, three input-output models were applied to synthetic oil fields to validate and compare them to each other. Numerical simulators (Eclipse and the IMEX) were used to generate synthetic field data (total liquid production and cumulative production data) to which the *lt*CRMP, CRMP, and ICRM were fitted. The *lt*CRMP, CRMP, and ICRM were validated for secondary recovery with Synfield-1(streak case). For the balanced waterflood like the streak case, the CRMP and ICRM parameters were insensitive to relaxing the constraints. By comparing the results (estimated parameters and regression fits) obtained by all three models in Synfield-1, it is clear that the *lt*CRMP and ICRM are attractive alternatives to CRMP. ICRM was also able to detect the presence of no-flow boundaries in Synfield-2. In Synfield-3 the presence of a transmissibility barrier could be inferred by low interwell connectivities calculated from the ICR model. Synfield-4 showed that interwell connectivities between newly introduced injectors and existing producers can be estimated solely by interwell-distance between well-pairs. Finally, in Synfield-5, the gains between existing producers and injectors remain constant with the introduction of new injectors, and future liquid production after adding new injectors could be plausibly predicted by the approximate gains.

Chapter 4: Uncertainty Quantification of the Model Parameters

Investigating the uncertainty of the resulting model parameters is necessary to determine the validity of a history match done by regression. Traditional reservoir models, consisting of hundreds of differential equations and using uncertain parameters such as permeability and porosity, are too complex for a simple statistical analysis (Weber, 2009). One can use Monte Carlo simulations to generate multiple realizations of the model and study the uncertainty in complex reservoir models such as Eclipse or the IMEX. Landa et al. (2005) used clustered computing techniques to analyze uncertainty in history-matching and forecasting. Sayarpour (2008) generated ensembles of history-matching results using the CRM to quantify uncertainty in porosity and residual oil and water saturations.

In this chapter, confidence intervals are established for model parameters (gains and time constants) estimated by both nonlinear and linear regression methods. This simple analysis of uncertainty in resulting model parameters does not require ensembles of models or history-matching solutions.

4.1 Confidence Intervals on Model Parameters with CRMP

As discussed in Chapter 3, the CRMP is highly nonlinear and is expressed in a recursive form. As a result of the nonlinear nature of the CRMP, direct estimation of confidence intervals on model parameters is quite difficult in practice. Weber (2009) suggested one way to establish confidence limits of gains by assuming that time constants

are not regression parameters, but constants. In this approach, the resulting model is linear in gains if producer BHPs are kept at constant value and the total production rate of a producer j at the time step k, q_{jk}, is expressed in terms of initial total production rate, q_{j0}, as the following:

$$q_{jk} = q_{j0}\left(e^{-\Delta t/\tau_j}\right)^k + \left(1-e^{-\Delta t/\tau_j}\right)\left[\begin{array}{l} \left\{\left(e^{-\Delta t/\tau_j}\right)^{k-1} i_{11} + \left(e^{-\Delta t/\tau_j}\right)^{k-2} i_{12} + \ldots + \left(e^{-\Delta t/\tau_j}\right) i_{1(k-1)} + i_{1k}\right\} f_{1j} + \\ \left\{\left(e^{-\Delta t/\tau_j}\right)^{k-1} i_{21} + \left(e^{-\Delta t/\tau_j}\right)^{k-2} i_{22} + \ldots + \left(e^{-\Delta t/\tau_j}\right) i_{2(k-1)} + i_{2k}\right\} f_{2j} + \ldots + \\ \left\{\left(e^{-\Delta t/\tau_j}\right)^{k-1} i_{(i-1)1} + \left(e^{-\Delta t/\tau_j}\right)^{k-2} i_{(i-1)2} + \ldots + \left(e^{-\Delta t/\tau_j}\right) i_{(i-1)(k-1)} + i_{(i-1)k}\right\} f_{(i-1)j} + \\ \left\{\left(e^{-\Delta t/\tau_j}\right)^{k-1} i_{i1} + \left(e^{-\Delta t/\tau_j}\right)^{k-2} i_{i2} + \ldots + \left(e^{-\Delta t/\tau_j}\right) i_{i(k-1)} + i_{ik}\right\} f_{ij} \end{array}\right] \quad (4.1)$$

The first term on the right-hand side of Equation 4.1 accounts for primary recovery and the second term accounts for secondary recovery.

The CRMP was applied on Synfield-1(see Figure 3.1), and 95% confidence limits on gains were calculated by assuming the time constants are not regression parameters. In this regression analysis, the number of data points fitted was 42. For each producer, the number of fitted parameters (gains) used was five. Therefore, the degrees of freedom used for both the t-test and the standard deviation estimate was 37.

The results show the 95% confidence limits of gains are narrow enough to conclude regression coefficients are statistically significant. Table 4.1 and Figure 4.1

show the 95% confidence intervals on the gains. The details of the calculation of confidence intervals are shown in Appendix B.

Table 4.1: 95% Confidence intervals on gains estimated by CRMP in Synfield-1

f_{ij}	I1	I2	I3	I4	I5
P1	0.892 ± 0.0389	0.588 ±0 .032	0.226 ± 0.041	0.213 ± 0.047	0.214 ± 0.044
P2	0.028 ± 0.009	0.031 ± 0.009	0.045 ± 0.012	0.182 ± 0.017	0.046 ± 0.013
P3	0.012 ± 0.009	0.198 ± 0.009	0.103 ± 0.012	0.057 ± 0.015	0.192 ± 0.017
P4	0.064 ± 0.014	0.182 ± 0.013	0.555 ± 0.019	0.503 ± 0.022	0.544 ± 0.021

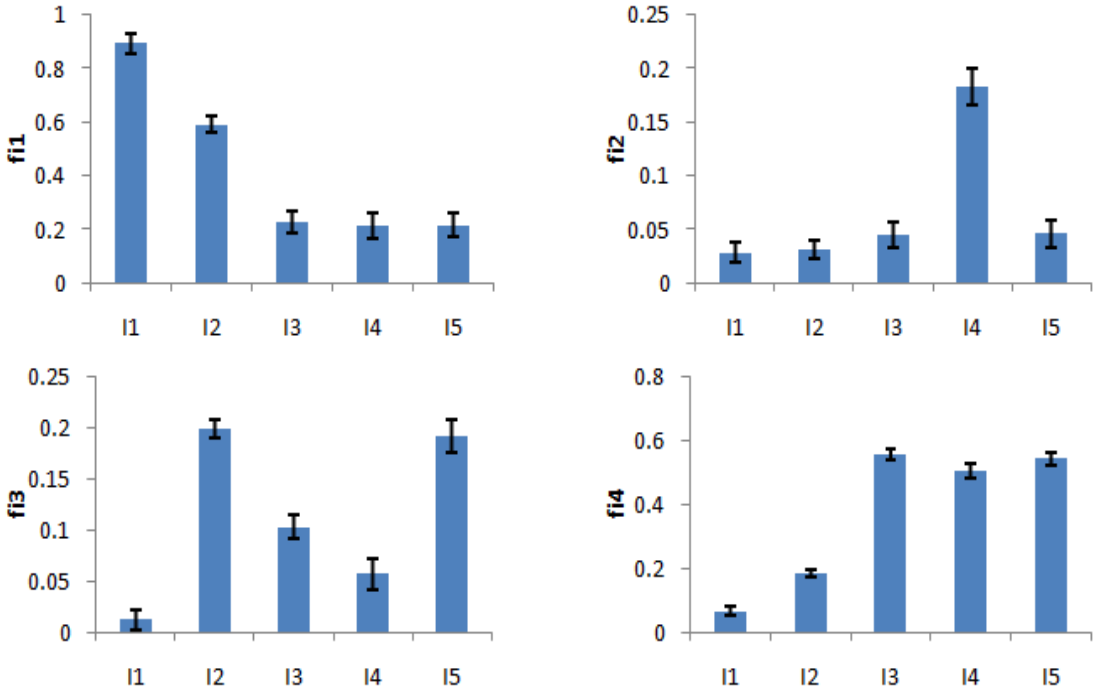

Figure 4.1: 95% confidence intervals on gains (f_{ij}) estimated by CRMP in Synfield-1 (streak case). Subscript i is an injector index in the range 1 to 5.

4.2 Confidence Intervals on Model Parameters with ICRM

As the CRMP is a nonlinear model, a straightforward statistical analysis of the variability of the parameter estimates is not possible (Weber, 2009). Assuming the time constants are not regression parameters allows us to establish the confidence limits on the gains; however, establishing the confidence limits for the time constants is still problematic with the CRMP. The linearity of ICRM makes it easy to establish confidence intervals of the model parameters (Montgomery and Peck, 1982).

The ICRM was applied on Synfield-1 (streak case), and 95% confidence limits on both the gains and time constants were calculated. The results show that the confidence limits of the gains calculated by the ICRM are smaller than those calculated by the CRMP (see Figure 4.2). This result is convincing evidence that regression coefficients (gains) estimated by the ICRM (linear model) are more statistically significant and reliable values than those estimated by the CRMP (nonlinear model). Figure 4.3 shows the 95% confidence intervals of the time constants. Since the value of zero is outside of the confidence interval, as shown in Figures 4.2 and 4.3, each fitted parameter is statistically different from zero to the confidence level (95% limit) assumed. Table 4.2 summarizes the 95% confidence intervals of the model parameters calculated by the ICRM.

Table 4.2: 95% confidence intervals on ICRM parameters in Synfield-1

f_{ij}	I1	I2	I3	I4	I5	τ_j (day)
P1	0.896 ± 0.018	0.593 ± 0.009	0.198 ± 0.017	0.252 ± 0.029	0.163 ± 0.024	5.16 ± 1.70
P2	0.036 ± 0.008	0.035 ± 0.003	0.040 ± 0.009	0.205 ± 0.012	0.033 ± 0.012	13.6 ± 4.78
P3	0.012 ± 0.005	0.181 ± 0.002	0.086 ± 0.005	0.040 ± 0.008	0.166 ± 0.007	12.3 ± 2.41
P4	0.059 ± 0.014	0.199 ± 0.006	0.663 ± 0.016	0.551 ± 0.024	0.593 ± 0.023	10.6 ± 1.56

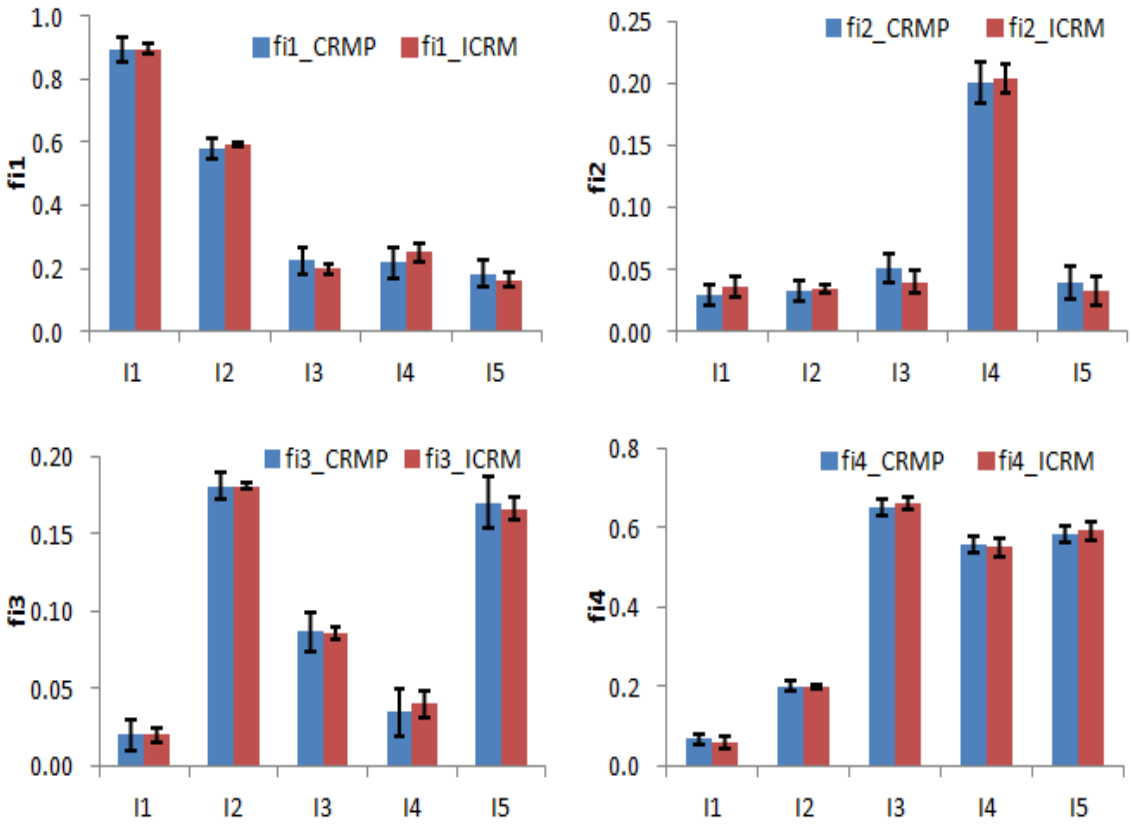

Figure 4.2: Comparison between CRMP gains (f_{ij}) and ICRM gains in Synfield-1 (streak case). 95% confidence intervals on gains (f_{ij}) estimated by the both CRMP and ICRM. Subscript i is an injector index in the range 1 to 5.

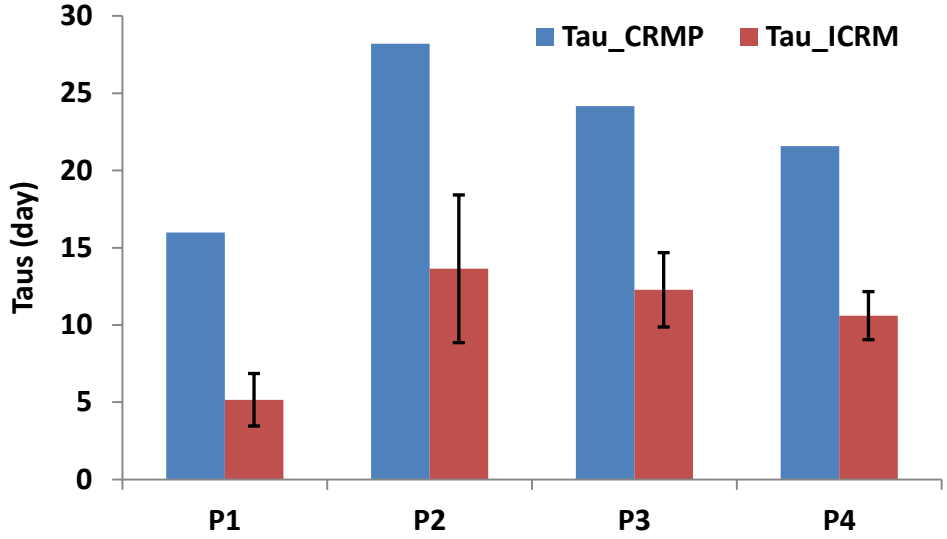

Figure 4.3: Comparison between CRMP time constants and ICRM time constants in Synfield-1 (streak case). 95% confidence intervals on time constants (τ_j) estimated by the ICRM. Subscript j is a producer index in the range 1 to 4.

4.3 Summary

In this chapter, I quantified the uncertainty inherent in the CRM and ICRM parameters and validated the trustworthiness of the model parameters. Assuming the time constants are not regression parameters allowed us to establish approximate confidence limits on the gains with the CRMP. The confidence limits of both the gains and time constants could be established easily with the ICRM. The 95% confidence limits of model parameters were narrow enough to conclude regression coefficients were statistically significant. Lastly, the confidence limits of the gains calculated by ICRM were smaller than those calculated by CRMP.

Chapter 5: Summary, Conclusions, and Recommendations for Future Work

The main objectives of this work were to develop and apply linearized capacitance-resistance models to waterfloods and to evaluate the uncertainty on model parameters. Therefore, two linear reservoir models (*lt*CRMP and ICRM) were developed and their applications in history-matching, convex optimization, and uncertainty quantification on model parameters were demonstrated.

This work developed and tested the *lt*CRMP and ICRM in several synthetic oil fields under waterflooding and showed that they were comparable in scope to the CRMP but allowed us to solving the objective functions analytically by matrix inversion. The relationship between interwell-connectivities and interwell-distance of well-pairs was presented. Also, the power of the ICRM permitted describing the interactions between newly introduced injectors and existing producers and predicting the future total liquid production based on these estimates.

5.1 Technical Contributions

The analytical solutions of the *lt*CRMP and ICRM for the drainage volume around each producer were developed in a similar manner as Sayarpour (2008). These two models are linear and provide advantages over the nonlinear waterflood model (CRMP): convex objective functions, efficient solution, and faster computation time in optimization.

The *lt*CRMP and ICRM were validated by applying them to five synthetic cases and comparing their results against simulated results. Each of these studies was selected to test different aspects of two models' capabilities. The streak case (Synfield-1) was used to test the two models' comparability in scope to the CRMP. Synfield-1 was also used to test the sensitivity of the CRMP and ICRM parameters to relaxing the constraints for the balanced waterflood.

The ICRM's capability in detecting the presence of transmissibility barriers was validated by applying it to two synthetic oil fields (Synfield-2 and Synfield-3). In the case studies with Synfield-4 and Synfield-5, the assumption that ICRM gains do not vary with the introduction of new injectors was verified and the prediction of future total liquid production based on interwell-distance gains was presented.

The streak case was also used to quantify the uncertainty on model parameters and establish the confidence intervals on the CRM gains and ICRM parameters.

5.2 Conclusions

All three simple reservoir models (CRMP, *lt*CRMP, and ICRM) presented in this work do not require a priori estimation of rock and fluid properties. Moreover, they share the similarities: the governing differential equation that describes the flow of the total fluid in oil reservoir and the number of model parameters in each model.

Two linear models (*lt*CRMP and ICRM) derived for secondary recovery in this work form convex objective functions and convex sets of constraints. Therefore, any local minimum found in optimization is the global minimum, thus uniqueness of a

solution is guaranteed always (see Appendix A). Linear formulation of these models allows us to solve convex objective functions analytically by matrix inversion if constraints are relaxed to get an approximate solution.

Application of *lt*CRMP and ICRM on synthetic oil fields (Synfields-1, 2, and 3) showed that estimated model parameters are consistent with the imposed geology. Both models were able to capture the general trends of reservoir production observed in synthetic reservoirs quite well. Therefore, *lt*CRMP and ICRM are attractive alternatives to CRMP. For the balanced waterflood like the streak case, the CRMP and ICRM parameters were insensitive to relaxing the constraints. In Synfield-4 the method to estimate the gains between well-pairs solely by interwell-distance between well-pairs (d_{ij}) for a homogeneous reservoir was demonstrated. In Synfield-5 the future total liquid production after adding new injectors could be plausibly predicted by interwell-distance dependent gains (f_{ij}^{d}). This method can guide decisions as to where to drill new injectors to increase future oil recovery and provide rapid solutions without having to run additional reservoir simulations for each scenario.

In Synfield-1 the uncertainty inherent in the CRM and ICRM parameters was quantified. Assuming the time constants are not known allowed us to establish approximate confidence limits on the gains with the CRMP. The confidence limits of both the gains and time constants could be established easily with the ICRM. The 95% confidence intervals of model parameters were narrow enough to conclude regression coefficients were statistically significant. Lastly, the confidence intervals of the gains

calculated by the ICRM were smaller than those calculated by the CRMP, suggesting that the ICRM is more precise than the CRMP.

5.3 Recommendations for Future Work

The following recommendations for future work are suggested.

1. All the models presented in this work have been derived based on black-oil reservoirs, which are relatively incompressible so one can assume numerous PVT related properties such as total compressibility (c_t), dissolved gas-oil ratio (R_s), oil formation volume factor (B_o), and gas formation volume factor (B_g), to be zero or constant. In this case, the use of static time constant and constant oil formation volume factor in the models is justified for waterflooded reservoirs.

   For a more compressible system (volatile oil or wet gas reservoir) or a field involving a gas flood (CO_2), the above assumptions are less valid, and space-time varying model parameters must be used in the models. If the bottom hole pressures (BHPs) are available and temperatures and API gravity factors around each well are specified or left as additional model parameters to be determined, the average reservoir pressures can be estimated from the models and used to estimate PVT related properties. This approach would greatly improve the robustness and accuracy of the model. However, the average reservoir pressures must be calculated implicitly, requiring iterations.

2. The objective functions presented in this work were solved to estimate model parameters by the means of the least mean squares (LMS). Therefore, new fitting

windows in regression must be chosen to include new production data if available in the future for each simulation. Model parameters can also be estimated by the recursive least squares (RLS) method that can monitor the change in geological properties, such as total compressibility, both in the history and in the future when new production data are available without having to select different fitting windows. We expect the RLS method can reflect the change in model parameters with respect to time and take into account dual role wells and wells shut-in for long time over the analyzed periods.

3. The new reservoir models developed in this thesis considered vertical wells. Further research to consider horizontal and inclined wells would verify that the models can be used effectively regardless of the types of well configurations.
4. Natural water influx into a hydrocarbon reservoir during pressure depletion is common. In this case, the waterflood is unbalanced, so we must take into account water influx as an additional independent variable in the model. The model estimation can be improved if pseudo steady-state aquifer models that were suggested by Walsh and Lake (2003) are used in the models.
5. Two simple reservoir models derived (*lt*CRMP and ICRM) have been only applied to synthetic oil fields in this work. Application of the models on real oil fields is strongly recommended to strengthen the validity of the models.
6. In this work, the gains between newly installed injectors and existing producers for a homogeneous reservoir could be approximated based on interwell-distance between well-pairs. This method is not well-suited for placing new producers. If

new producers are added in a reservoir, the gains between existing injectors and producers that are calculated by regression prior to adding new producers will change significantly. Further research should investigate simple methods that can approximate the gains between existing producers and injectors after adding new producers in a reservoir.

7. Approximate gains (f_{ij}^{d}) based on interwell-distance between well-pairs can be combined with an oil fractional-flow model and an economic model to determine where to drill new injectors to maximize the net present value of future oil recovery. A case study to determine optimal injector locations using this methodology is recommended.
8. The current models (CRM, *lt*CRMP, and ICRM) need historic water injection rates (or cumulative injection) and producers BHPs for history-matching of total liquid production rates (or cumulative total liquid production). Geoscientists can manipulate future injection rates and producers BHPs to provide the best excitation signal for fitting the models to resulting production data. There may be an optimal way to perturb injection rates and producer BHPs to get a robust signal for model fitting.

Appendix A: Convex Optimization with Linear CRMs

For a linear or nonlinear programming problem called the *convex programming problem*

$$\text{Minimize: } f(\mathrm{x})$$

$$\text{Subject to: } g_i(\mathrm{x}) \le 0 \quad i=1, \ldots, m \tag{A-1}$$

in which (a) *f (x)* is a convex function, and (b) each inequality constraint is a convex function (so that the constraints form a convex set), then the local minimum of *f (x)* is also the global minimum (Edgar et al., 2001). The objective function of CRM optimization with linear water flooding predictive models, such as ICRM and *lt*CRMP, is a convex function. According to the definition of *convex programming problem*, the local minimum found from an objective function is also the global minimum if the constraints associated with the model form a convex set. The constraints associated with ICRM are all linear, forming a straightforward convex set. The constraints associated with *lt*CRMP are nonlinear; however, they also form a convex set.

Suppose there are *n* injectors and two producers (P1 and P2) in water floods and assume there are no sealing faults in a reservoir. With *lt*CRMP, Equations A-2 to A-4 show the constraints regarding injector I1 to be:

$$\frac{f_{11}^{'}}{1-e_1} + \frac{f_{12}^{'}}{1-e_2} \le 1 \tag{A-2}$$

$$f_{11}^{'},\ f_{12}^{'} \ge 0 \tag{A-3}$$

$$0 \le e_1,\ e_2 \le 1 \tag{A-4}$$

where f'_{11} is the fraction of water rate from injector I1 flowing towards producer P1 accounting for time lag (1-e_1), f'_{12} is the fraction of water rate from injector I1 flowing towards producer P2 accounting for time lag (1-e_2), e_1 is $exp(-\Delta t/\tau_1)$, and e_2 is $exp(-\Delta t/\tau_2)$.

A set of points x satisfying the following relation is convex if the Hessian matrix (or simply Hessian) H(x) is a real symmetric positive-semidefinite matrix.

$$x^T H(x) x \leq 1 \tag{A-5}$$

H(x) is another symbol for $\nabla^2 f(x)$, the matrix of second partial derivative of $f(x)$ with respect to each x_i (Edgar et al., 2001). The Hessians of Equations A-3 and A-4 are zeros indicating Equations A-3 and A-4 are both convex and concave functions. The Hessian of Equation A-2 is shown as the following:

$$H(f'_{11}, f'_{12}, e_1, e_2) = \begin{bmatrix} 0 & 0 & \frac{1}{(1-e_1)^2} & 0 \\ 0 & 0 & 0 & \frac{1}{(1-e_2)^2} \\ \frac{1}{(1-e_1)^2} & 0 & \frac{2f'_{11}}{(1-e_1)^3} & 0 \\ 0 & \frac{1}{(1-e_2)^2} & 0 & \frac{2f'_{12}}{(1-e_2)^3} \end{bmatrix} \tag{A-6}$$

If the principal minors of Equation A-6 are equal or greater than zero at any value of parameters (f'_{11}, f'_{12}, e_1, e_2), then the Hessian is positive-definite, and Equation A-2 is convex. If the principal minors of Equation A-6 are equal or less than zero at any value of parameters (f'_{11}, f'_{12}, e_1, e_2), then the Hessian is negative-definite, and Equation A-2 is concave. For this example, the principal minors of $H(f'_{11}, f'_{12}, e_1, e_2)$ are all zeros except M_{44}, which is the principal minor of a 4×4 matrix from Equation A-6. M_{44} is found to be

$(1-e_1)^{-4}(1-e_2)^{-4}$, so M_{44} is always positive. This result indicates the effective gains (f'_{11} and f'_{12}) are irrelevant in determining the convexity of Equation A-2. Therefore, all the constraints (Equations A-2, A-3, and A-4) are convex, and they form a convex set. There will be another convex set, which is formed by set of constraints due to injector I02.

Now, suppose there are *n* injectors and three producers (P1, P2, and P3). Equations A-7 to A-9 show the constraints regarding injector I1 to be:

$$\frac{f'_{11}}{1-e_1}+\frac{f'_{12}}{1-e_2}+\frac{f'_{13}}{1-e_3}\le 1 \tag{A-7}$$

$$f'_{11},\, f'_{12},\, f'_{13}\ge 0 \tag{A-8}$$

$$0<e_1,e_2,e_3\le 1 \tag{A-9}$$

Equations A-8 and A-9 are both concave and convex, and the Hessian matrix of Equation A-7 is shown below:

$$H(f'_{11},f'_{12},f'_{13},e_1,e_2,e_3)=\begin{bmatrix} 0 & 0 & 0 & \frac{1}{(1-e_1)^2} & 0 & 0 \\ 0 & 0 & 0 & 0 & \frac{1}{(1-e_2)^2} & 0 \\ 0 & 0 & 0 & 0 & 0 & \frac{1}{(1-e_3)^2} \\ \frac{1}{(1-e_1)^2} & 0 & 0 & \frac{2f'_{11}}{(1-e_1)^3} & 0 & 0 \\ 0 & \frac{1}{(1-e_2)^2} & 0 & 0 & \frac{2f'_{12}}{(1-e_2)^3} & 0 \\ 0 & 0 & \frac{1}{(1-e_3)^2} & 0 & 0 & \frac{2f'_{13}}{(1-e_3)^3} \end{bmatrix} \tag{A-10}$$

The principal minors of Equation A-10 are all zeros except M_{66}, which is the principal minor of a 6×6 matrix from Equation A-10. M_{66} is found to be

$(1-e_1)^{-4}(1-e_2)^{-4}(1-e_3)^{-4}$, so M_{66} is always negative. Therefore, all the constraints (Equations A-7 to A-9) are concave, and they also form a convex set. There are the constraints regarding other injectors; however, these constraints form convex sets as well by induction.

Appendix B: Establishment of Confidence Intervals on Fitted Parameters

To establish the confidence intervals about the fitted parameters, the sum of the squares of the fitted function from the actual data points is defined first as the following Equation B-1,

$$S_r = \sum_{i=1}^{N} (f_i - f(x_i, y_i))^2 \tag{B-1}$$

where S_r is the sum of the squared residuals, f_i is the actual (or measured) data points, and $f(x_i, y_i)$ is the proposed linear regression function with two independent variables (x and y) evaluated at the i^{th} x and y values (Ludovice, 2003). Next, the effective standard deviation about a regression curve is calculated by Equation B-2,

$$S_{y/x} = \sqrt{\frac{S_r}{N-m}} \tag{B-2}$$

where, $S_{y/x}$ is the standard error, S_r is defined by Equation B-1, N is the total number of data points, and m is the total number of coefficients in the fitted equation (Ludovice, 2003).

To construct confidence intervals about the fitted parameters, the inverse of the covariance matrix C is defined by Equation B-3,

$$C^{-1} = \left[Z^T Z \right]^{-1} \tag{B-3}$$

where C^{-1} is the inverse of covariance matrix C and Z is the matrix that consists of M columns, one for each coefficient in the proposed regression function, and N rows, one

for each of the data points. Z^T is the transpose of the matrix in which the rows and columns are switched (Ludovice, 2003).

Finally, the 95% confidence interval about a fitted parameter is given below as a function of the variance value (C_{ii}) for that coefficient and the standard error of fit:

$$a_i \pm t_{0.95}(\nu = N - m) S_{y/x} \sqrt{C_{ii}^{-1}} \tag{B-4}$$

where a_i is a fitted parameter, $t_{0.95}(\nu = N - m)$ is the student's t-distribution at 95% confidence limits in which ν is the degree of freedom, and $\sqrt{C_{ii}^{-1}}$ is the square root of the off-diagonal elements of C^{-1} (Ludovice, 2003).

Nomenclature

L, F, t mean length, force, and time, respectively.

BHP = bottom hole pressure (F/L^2)

C = covariance matrix

C^{-1} = inverse of covariance matrix C

CM = capacitance model

CMG = computer modeling group Ltd.

CRM = capacitance-resistive model or capacitance-resistance model

CRMP = a producer-based representation of capacitance-resistance model

CWI = cumulative water injection (L^3)

c_t = total reservoir compressibility (L^2/F)

d_{ij} = interwell-distance between injector-producer well-pair (L)

f_{ij} = fraction of injection from injector i flows to producer j, dimensionless

f_{ij}^{d} = interwell-distance dependent *gain*, dimensionless

ICRM = integrated capacitance-resistance model

i = water injection rate (L^3/t)

IMEX = Implicit-explicit black oil simulator

J = productivity index ($L^5/F\text{-}t$)

LMR = linear multivariate regression

*lt*CRMP = linearly transformed CRMP

*lt*CRM = linearly transformed CRM

MLP = multiple linear regression

n_p = total number of producers

n_t = total number of historic time periods

N_i = total number of injectors

N_p = cumulative total production (L^3)

OOIP = original oil in place (L^3)

P = pressure (F/L^2)

P_{wf} = bottom-hole pressure (F/L^2)

q = total liquid production rate (L^3/t)

R^2 = correlation coefficient

S_r = sum of the squared residuals (L^6/t^2 or L^6)

$S_{y/x}$ = effective standard deviation about a regression curve (L^3/t or L^3)

t = time (t)

$t_{0.95}$ = student's t-distribution at 95% confidence limits

V_p= pore volume (L^3)

Greek alphabets

τ = time constant (t)

ξ = integrating variable (t)

Subscripts and superscripts

cal = calculated quantity by the model

hi = highest

i = injector index

ij = injector-producer pair index

j = producer index

k = time step index

lo = lowest

obs = observed quantity

0 = initial time step

References

Albertoni, A. and Lake, L.W. 2003. "Inferring Connectivity Only From Well-Rate Fluctuations in Waterfloods." *SPE Reservoir Evaluation and Engineering Journal*, **6** (1): 6-16.

Aziz, K. and Settari, A. 1979. *Petroleum Reservoir Simulation*. London: Elsevier Applied Science Publishers.

Barros-Griffiths, I. 1998. "The Extreme Spearman Rank Correlation Coefficient in the Characterization of the North Buck Draw Field." M.S. Thesis, The University of Texas at Austin, Austin, Texas.

Buckley, S.E. and Leverett, M.C. 1942. "Mechanics of Fluid displacement in Sands." *Trans*., AIME 146: 107-116.

De Sant' Anna Pizarro, J.O. 1998. "Estimating Injectivity and Lateral Autocorrelation in Heterogeneous Media." Ph.D Dissertation, The University of Texas at Austin, Austin, Texas.

Dykstra, H. and Parsons, R.L. 1950. "The Prediction of Oil Recovery by Waterflood. Paper presented at Secondary Recovery of Oil in the United States." API, Dallas, Texas, 160-174.

Edgar, T.F., Himmelblau, D.M., and Lasdon, L.S. 2001. *Optimization of Chemical Processes*. 2nd Ed. New York: McGraw-Hill Companies, Inc., Ch. 4, p. 123-127.

Landa, J. et al. 2005. "History-matching and Associated Forecast Uncertainty Analysis-Practical Approaches Using Cluster Computing." Paper IPTC 10751 presented at the International and Productoin Rates. Paper SPE 121353 presented at the SPE Western Regional Meeting, San Jose, California, 24-26 March.

Liang, X., Weber, B., Edgar, T.F., Lake, L. W., Sayarpour, M., and Yousef, A.A. 2007. "Optimization of Oil Production in a Reservoir Based on Capacitance Model of Production and Injection Rates." Paper SPE 107713 presented at the SPE Hydrocarbon Economics and Evaluation Symposium, Dallas, Texas, 1-3 April.

Ludovice, P.J. 2003. "Generalized Least-Squares Regression." *Statistics Handout*, Georgia Institute of Technology, Atlanta, Georgia.

Montgomery, D.C. and Peck, E.A. (1982). *Introduction to Linear Regression Analysis*. John Wiley & Sons, Ch.4, p. 124-141.

Nguyen, A.N., Kim, J.S., Lake, L.W., Edgar, T.F., and Haynes, Byron (2011). "Integrated Capacitance-Resistive Model for Reservoir Characterization in Primary and Secondary Recovery." Paper SPE 147344 presented at the SPE Annual Technical Conference and Exhibition, Denver, Colorado, 30 October-2 November.

Panda, M.N. and Chopra, A.K. 1998. "An Integrated Approach to Estimate Well Interactions." Paper SPE 39563 presented at the SPE India Oil and Gas Conference and Exhibition, New Delhi, India, 17-19 February.

Refunjol, B.T. and Lake, L.W. 1999. "Reservoir Characterization Based on Tracer Response and Rank Analysis of Production and Injection Rates." *In Reservoir Characterization Recent Advance*, ed. R. Schatzinger and J. Jordan, Ch.15, p. 209-218, AAPG Memoir 71.

Sayarpour, M., Zuluaga, E., Kabir, C.S., and Lake, L.W. 2007. "The Use of Capacitance-Resistive Models for Rapid Estimation of Waterflood Performance and Optimization." Paper SPE 110081 presented at the SPE Annual Technical Conference and Exhibition, Anaheim, California, 11-14 November.

Sayarpour, M. 2008. "Development and Application of Capacitance-Resistive Models in Water/CO_2 Floods." Ph.D. Dissertation, The University of Texas at Austin, Austin, Texas.

Seborg, D., Edgar, T.F., and Mellichamp, D. 2010. *Process Dynamics and Control*. 3rd Ed. John Wiley & Sons, Ch.2, p.25.

Stiles, W.E. 1949. "Use of Permeability Distribution in Waterflood Calculations." *Trans*., AIME 186: 9-13.

Soeriawinata, T., Kelkar, M., "Reservoir Management Using Production Data." Paper SPE 52224 presented at the 1999 SPE Mid-Continent Operation Symposium, Oklahoma City, Oklahoma, 28-31 March.

Thompson, M., 2006. *Intuitive Analog Circuit Design*. Elsevier E-Book, Ch 2, p.16.

Walsh, M.P. and Lake, L.W. 2003. *A Generalized Approach to Primary Hydrocarbon Recovery*. Handbook of Petroleum Exploration and Production, 4 series ed. J. Cubbitt. Elsevier. Amsterdam.

Weber, D. 2009. “The Use of Capacitance-Resistive Models to Optimize Injection Allocation and Well Location in Water Floods.” Ph.D. Dissertation, The University of Texas at Austin, Austin, Texas.

Weber, D., Edgar, T.F., Lake, L.W., Lasdon, L., Kawas, S., and Sayarpour, M. 2009. “Improvements in Capacitance-Resistive Modeling and Optimization of Large Scale Reservoirs.” Paper SPE 121299 presented at the SPE Western Regional Meeting, San jose, California, 24-26 March.

Welge, H.J. 1952. “A Simplified Method for Computing Oil Recovery by Gas or Water Drive.” *Trans*. AIME 195: 91-98.

Yousef, A.A., Gentil, P.H., Jensen, J.L. and Lake, L.W. 2006. “A Capacitance Model to Infer Interwell Connectivity from Production and Injection Rate Fluctuations.” *SPE Reservoir Evaluation & Engineering*, **9** (5): 630-646.

Vita

Jong Suk Kim was born in Seoul, South Korea. He received the degree of Bachelor of Science in Chemical and Biomolecular Engineering from Georgia Institute of Technology, Georgia. After completion of his Bachelor's degree, he worked for a half year in Samsung Engineering as a researcher and a process engineer. In August, 2009, he started his graduate program in the department of Chemical Engineering at the University of Texas at Austin.

Email: jkim0916@gmail.com

This thesis was typed by the author.